PERGAMON

Journal of Structural Geology 22 (2000) 349–371

JOURNAL OF STRUCTURAL GEOLOGY

www.elsevier.nl/locate/jstrugeo

Stress and fluid control on décollement within competent limestone

Antonio Teixell[a,*], David W. Durney[b], Maria-Luisa Arboleya[a]

[a]*Departament de Geologia, Universitat Autònoma de Barcelona, 08193 Bellaterra, Spain*
[b]*Department of Earth and Planetary Sciences, Macquarie University, Sydney, NSW 2109, Australia*

Received 5 October 1998; accepted 23 September 1999

Abstract

The Larra thrust of the Pyrenees is a bedding-parallel décollement located within a competent limestone unit. It forms the floor of a thrust system of hectometric-scale imbrications developed beneath a synorogenic basin. The fault rock at the décollement is a dense stack of mainly bedding-parallel calcite veins with variable internal deformation by twinning and recrystallization. Veins developed as extension fractures parallel to a horizontal maximum compressive stress, cemented by cavity-type crystals. Conditions during vein formation are interpreted in terms of a compressional model where crack-arrays develop at applied stresses approaching the shear strength of the rock and at fluid pressures equal to or less than the overburden pressure. The cracks developed in response to high differential stress, which was channelled in the strong limestone, and high fluid pressure in or below the thrust plane. Ductile deformation, although conspicuous, cannot account for the kilometric displacement of the thrust, which was mostly accommodated by slip on water sills constituted by open cracks. A model of cyclic differential brittle contraction, stress reorientation, slip and ductile relaxation at a rheological step in the limestone is proposed as a mechanism for episodic décollement movement. The model accounts for the peculiar microstructural character of the fault zone, for alternating sequences of bedding-parallel shortening (leading to crack dilation) and bedding-parallel shear (leading to décollement slip) and for hanging wall imbrication consequent upon décollement slip.

1. Introduction

In external thrust systems of orogenic belts, the rheology of lithic units exerts a primary control on the structural characteristics of the system, i.e. thrust ramp attitude and spacing, and especially the location of décollement levels (Woodward and Rutherford, 1989, and references therein). Bedding décollements in upper crustal stratified rocks are usually found in lithologically weak units, or near the interface of these and more competent layers (e.g. Buxtorf, 1916; Rich, 1934; Rodgers, 1949; Ramsay and Huber, 1987, p. 518). Classic representatives include easily deformed evaporites or water-releasing rocks, such as shales or siltstones. In these cases, there is an obvious lithologic reason for reduced strength, and yield can be either brittle (e.g. in overpressured shales), ductile (in salt and other evaporitic rocks), or a combination of both (Hubbert and Rubey, 1959; Davis and Engelder, 1985, etc.). Nevertheless, rare examples of décollement overthrusts developed within competent units, in preference to apparently weaker layers nearby, have been reported (Pierce, 1957; Burchfiel et al., 1982; Coleman and Lopez, 1986; Woodward and Rutherford, 1989). In such examples, in the absence of an obvious lithologic cause, it is assumed that strong units had concentrated stress, and high fluid pressures are generically invoked, but explanations of how and why the décollement formed there are lacking. These 'strong' décollements stand as one of the major problems in thrust tectonics.

In this work we describe a décollement thrust, called

* Corresponding author.
E-mail address: geotec@geologia.uab.es (A. Teixell).

0191-8141/00/$ - see front matter
PII: S0191-8141(99)00159-5

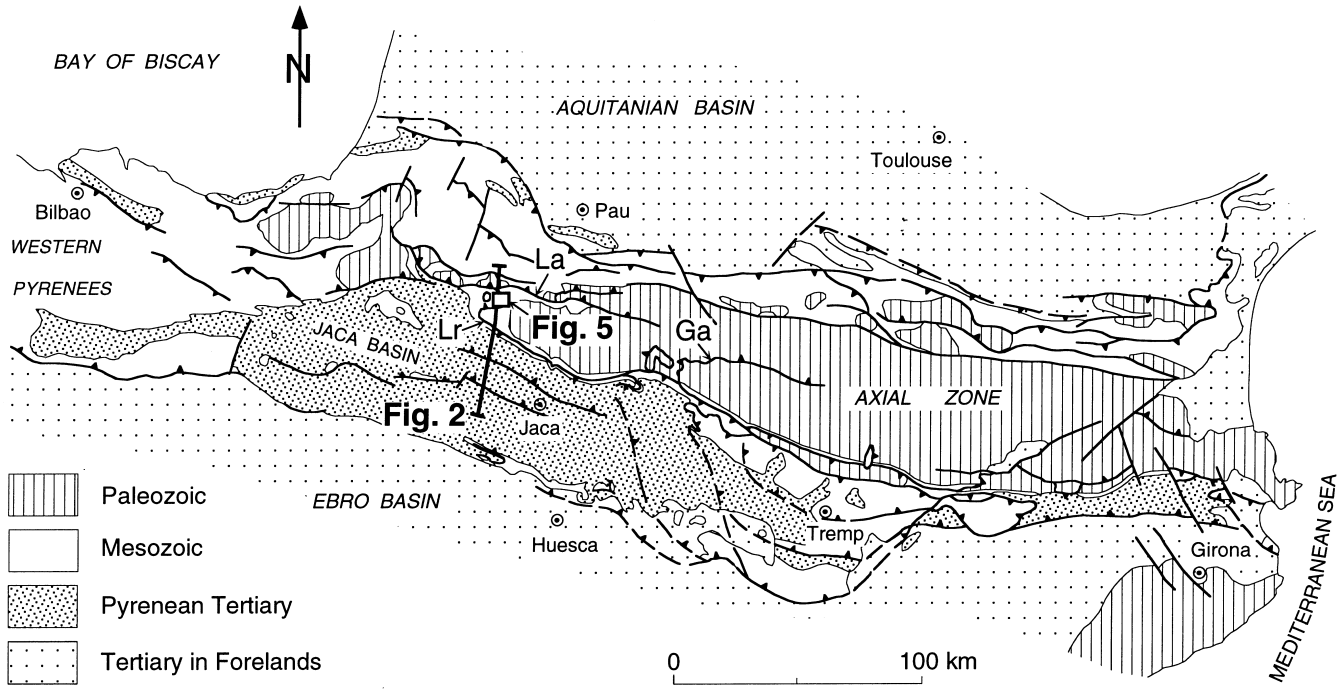

Fig. 1. Tectonic map of the Pyrenees showing location of the study area (Fig. 5) in the south-vergent belt of the orogen. Lr: Larra thrust; La: Lakora thrust; Ga: Gavarnie thrust.

the Larra thrust, which occurs within a competent limestone unit of the southern Pyrenees. Rheological weakness and water-generating capacity of the host rock were not primary causes for detachment. The thrust zone is characterized by a dense stack of mainly bedding-parallel calcite veins, which exhibit moderate ductile deformation and recrystallization features. We first describe the detailed structural characteristics of

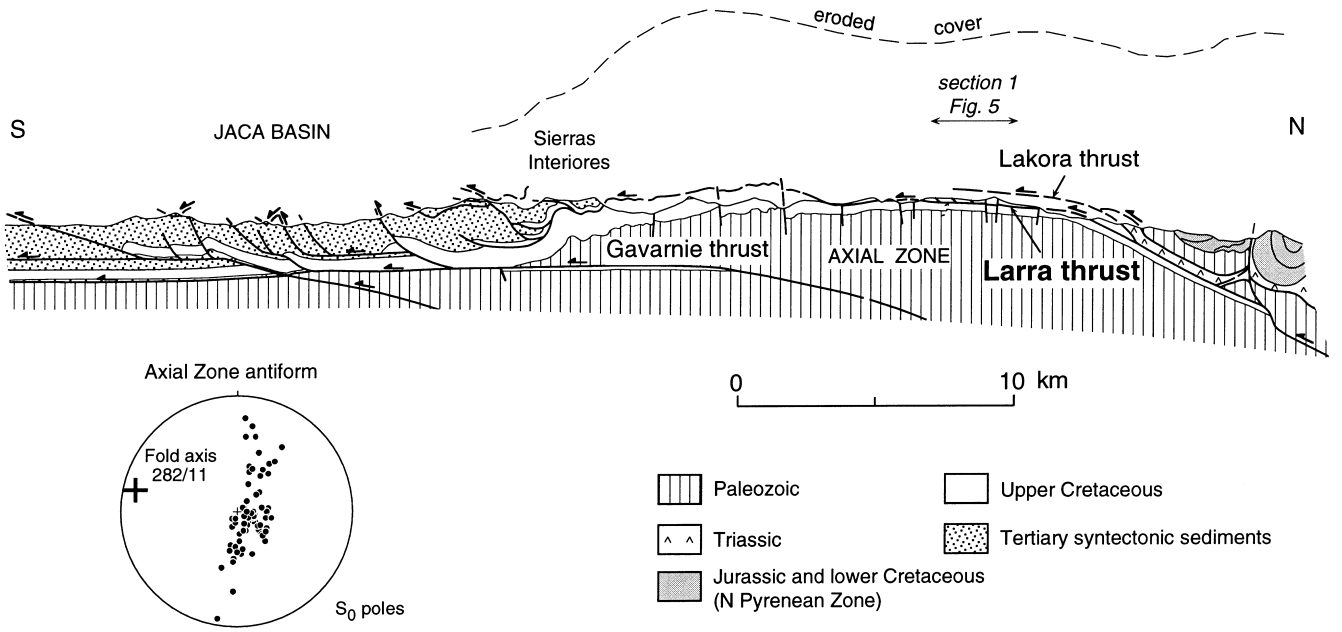

Fig. 2. Regional cross-section of the west-central Pyrenees (location in Fig. 1) showing the structural setting of the Larra thrust study area (after Teixell, 1992). Stereoplot represents bedding surfaces (S_0) in Cretaceous rocks of the Axial Zone cover and defines the hanging wall anticline of the Gavarnie thrust. (Lower hemisphere, equal-area projection in this and other diagrams.)

the décollement fault zone and associated ramps and the microstructure of the fault rock. Guided by these observations, mechanical considerations lead to a new concept for fault localization and movement in rheologically strong units where localized weakening is induced by stress and fluid channelling. Fluctuating cycles of fluid-assisted yield and stress reorientation determined the décollement evolution.

2. Regional tectonic setting

The Pyrenees is a Cenozoic orogenic belt that formed at the collisional boundary between the Iberian and European plates. It is dominated by fold-and-thrust structures, which involve both a Hercynian (Paleozoic) basement and Mesozoic–Cenozoic cover strata (Fig. 1). Thrust faults form ramps in basement rocks, that turn into bedding décollements at the base of the cover, usually in a Triassic gypsum–shale unit (Keuper facies) (Séguret, 1972). The Larra thrust is one of the higher thrusts in the south-vergent belt of the west-central Pyrenees. It affects Upper Cretaceous to Eocene rocks over a N–S distance of more than 20 km in a topographically high part of the Pyrenean chain, from the northern Axial Zone to the Sierras Interiores range (Figs. 1 and 2) (Teixell, 1990, 1996). For most of its extent, the Larra thrust is a bedding décollement within basal Upper Cretaceous limestone that forms the western cover of the Axial Zone basement massif. Triassic rocks, the common décollement level in the Pyrenees, are absent in this area; Upper Cretaceous strata rest with angular unconformity directly on Devonian and Carboniferous rocks. At its northern, trailing edge, the Larra thrust branches from the Lakora thrust, one of the major Pyrenean basement-involved faults (Fig. 2). To the south, it climbs to younger Cretaceous shales in the Sierras Interiores area (Labaume et al., 1985) (Fig. 2). The leading edge, which was probably blind, is located in Eocene synorogenic flysch of the Jaca basin (Fig. 1). For its entire length, the Larra thrust forms the floor of a system of hectometric-(100 m) scale imbrications which show a cumulative displacement of ca. 5 km (Teixell, 1992). Regional transport direction in the southern Pyrenees is to the SSW, approximately N200 (Séguret, 1972), but local departures from this direction, notably to the SW, were found in the course of this study.

Syntectonic sediments indicate that the Larra thrust formed during the Middle Eocene as a footwall splay of the older Lakora thrust (Teixell, 1992, 1996). Reconstruction of the eroded material overlying these structures indicates that, during thrusting, the Cretaceous limestone was buried under some 6–7 km of overburden (Fig. 2) corresponding to the thin leading edge of the Lakora thrust sheet and the northern

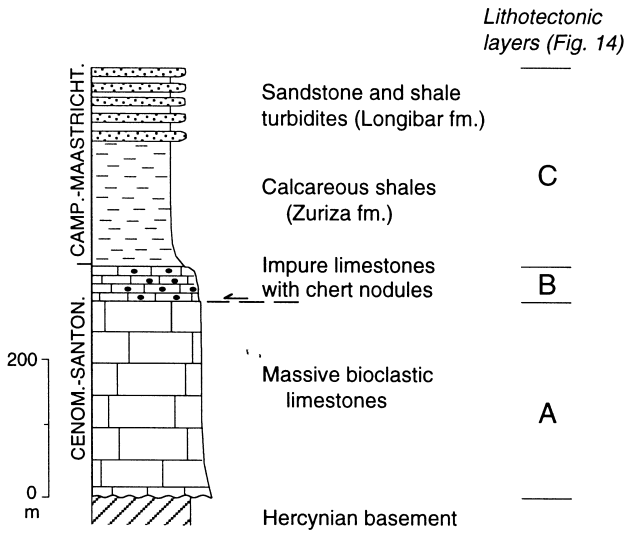

Fig. 3. Simplified stratigraphic column of the Upper Cretaceous of the northern Axial Zone, showing position of the Larra décollement thrust.

extension of the Eocene synorogenic basin. Preliminary illite 'crystallinity' investigations by J. Bastida (Univ. de València) in marls directly above the limestone (seven measurements using a grain size fraction $< 2\,\mu m$) yield Kubler index values ($\Delta 2\theta$) ranging from 0.19 to 0.26°. This is indicative of peak metamorphic conditions in the uppermost anchizone to the lower epizone (~prehnite–pumpellyite to greenschist transition). It should be noted that this estimate (about 300°C) is higher than that calculated from depth of burial (≥ 200°C). Present exposure of the Larra thrust is due to the fact that, subsequent to thrusting, the region was folded and uplifted by the Axial Zone antiformal culmination, related to the deeper-seated Gavarnie basement-involved thrust (Fig. 2). The culmination has a westerly plunge of 11°, causing termination of the Axial Zone Paleozoic outcrops in the vicinity of the study area. High-angle normal faults formed in the antiform crest, in association with this late deformation, and their accompanying minor structures overprint the Larra thrust mesostructural development. Based on the relationships with syntectonic sediments in the Jaca basin, the Gavarnie deformation can be ascribed to the Late Eocene–Early Oligocene (Teixell, 1992).

The Larra thrust and overlying imbrications are analysed at various localities on the northern limb of the Axial Zone antiform, a mountainous area, ca. 2000 m above s.l., where vigorous relief and sparse vegetation provide excellent exposure. It is in this area where the décollement is located in the competent Cretaceous limestone, constituting the objective of the study.

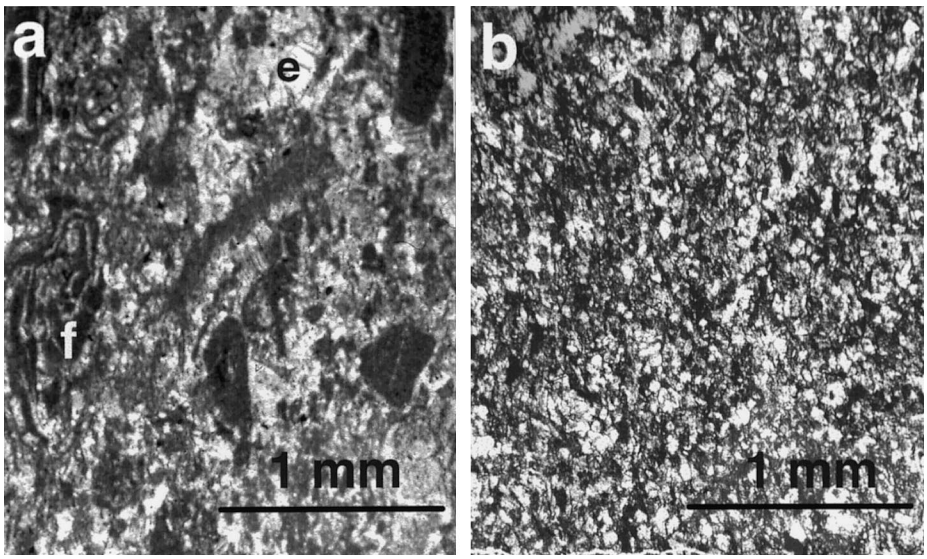

Fig. 4. Photomicrographs of limestone protoliths of the Larra thrust. (a) Bioclastic grainstone pertaining to the massive limestone below the thrust zone (lithotectonic unit A), with echinoderm ossicles (e) and micritized carbonate components (peloids and foraminifera, f). Plane-polarized light (PPL). (b) Fine-grained silty/sandy grainstone–packstone of the bedded limestone above the thrust zone (lithotectonic unit B), with rounded grains of quartz (white). PPL. Cleavage in both samples is vertical, (a) has a grain-alignment fabric (type 1 of Durney and Kisch, 1994) and the rock in (b) usually shows rough and spaced cleavages.

2.1. Local stratigraphy

At its western termination, the Hercynian basement consists essentially of weakly metamorphosed slates and turbiditic sandstone–shale alternations (with minor limestone) attributed to the Devonian–Carboniferous (Mirouse, 1966). Hercynian deformation consists of NW–SE-trending folds with accompanying slaty cleavage. A cross-cutting E–W cleavage related to Alpine deformation is also present. It is thus likely that the fine-grained Paleozoic rocks were less competent than the overlying Cretaceous limestone.

The stratigraphy of the Upper Cretaceous rocks northwest of the Axial Zone has been described by Ribis (1965) and Teixell (1992). The lower part is composed of Cenomanian–Santonian limestone (referred to in the literature as 'calcaires des cañons'), overlain by the Zuriza shales and then by the Longibar turbiditic series, both of Campanian–Maastrichtian age (Fig. 3). The limestone in turn consists of two members (Fig. 3): a lower unit of massive micritic and bioclastic limestone (Cenomanian–Lower Santonian, 280–300 m), and an upper part composed of well-bedded impure limestone (Upper Santonian, 30–50 m). The lower, massive unit consists of wackestones and bioclastic grainstones–packstones composed of peloids (micritized grains) and fragments of rudists, echinoderms, and foraminifera (lacazinids and miliolids) (Fig. 4a). The upper, bedded unit is made up of notably finer-grained wackestones–packstones with disseminated silt and fine quartz sand (Fig. 4b). It also contains micritized carbonate components and occasional echinoid and foraminifera remains, and locally displays abundant chert nodules. No shaly interlayer is found at the boundary between the lower and the upper limestone members, but the top of the upper limestone member grades vertically into Campanian calcareous shales of the Zuriza Formation. The overlying turbidites are overridden by the Lakora nappe, but in areas farther to the south the Upper Cretaceous is succeeded by up to 4500 m of Tertiary flysch (Fig. 2).

3. Local thrust system structure

On the northern limb of the Axial Zone antiform, the Larra thrust system is a thin imbricate fan composed of numerous south-vergent ramps that root in a bedding-parallel floor thrust (Larra thrust) (Fig. 5). Transport directions vary between N–S and NE–SW, as indicated by the structural trends of ramps and by stylolite and vein kinematic indicators. In the study area, the Larra thrust is located precisely at the boundary between the lower, massive limestone member and the upper, bedded impure limestone member of the Cenomanian–Santonian limestone (Teixell, 1990). It fits the strict definition of a décollement: a bedding-parallel slip plane without repetition of stratigraphy. Individual ramps cut the bedded limestones and the Zuriza shales. There is no evidence of major shear or décollement at the Paleozoic/Cretaceous unconformity or at the limestone/shale boundary. The footwall of the Larra décollement thrust is a tabular limestone body unaffected by folds and thrusts (Fig. 5), although

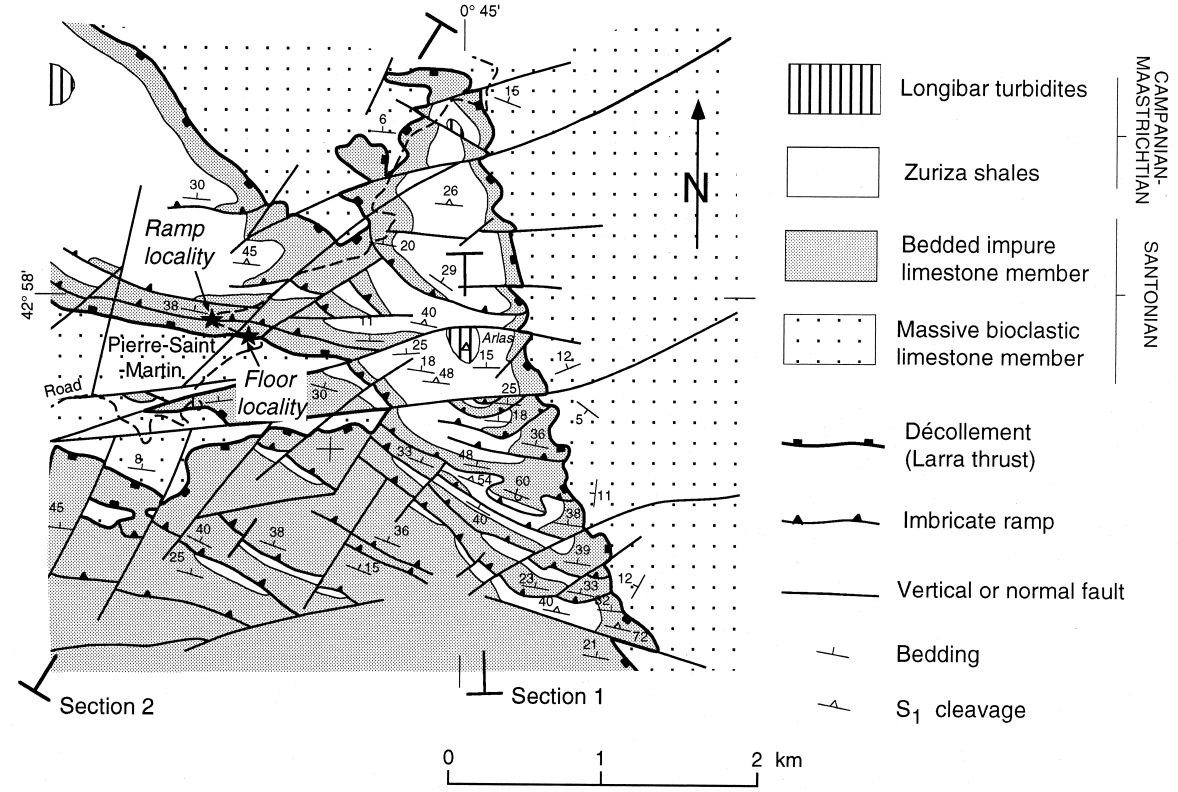

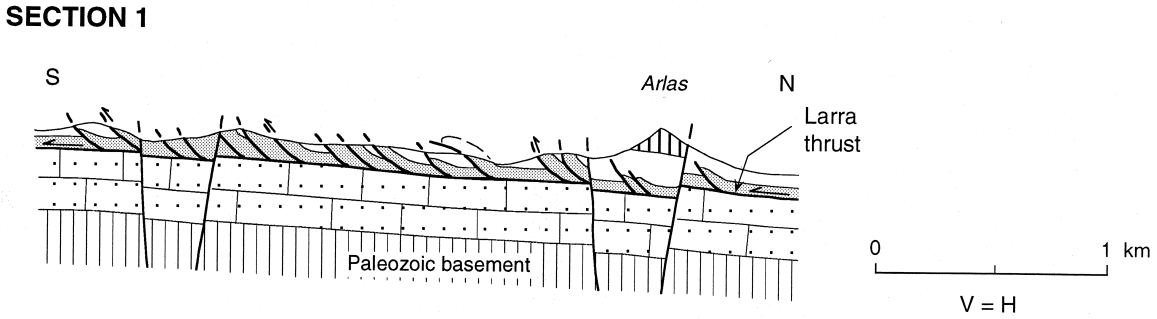

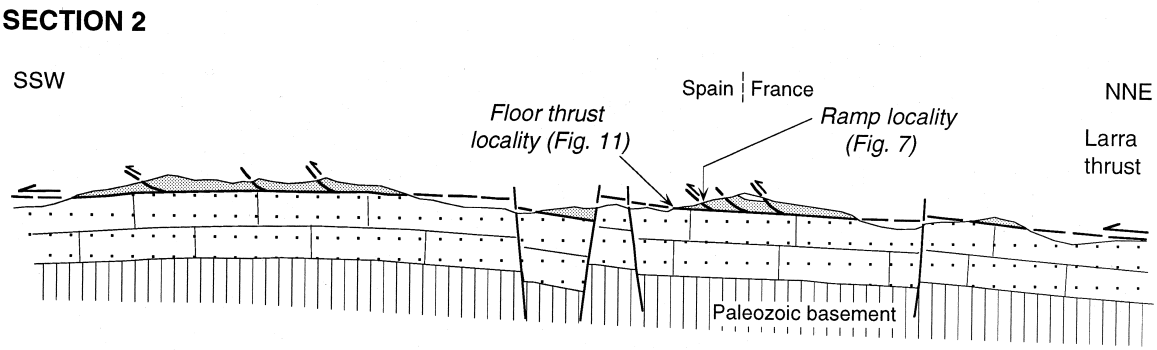

Fig. 5. Geological map and cross-sections of a segment of the Larra thrust system in the northern Axial Zone region (see location in Figs. 1 and 2) (modified after Teixell, 1990). The ramp and floor thrust (décollement) localities at Pierre-Saint-Martin are indicated. The Refugio de Belagua ramp fold (see description in text) is located some 5 km to the SW along the road.

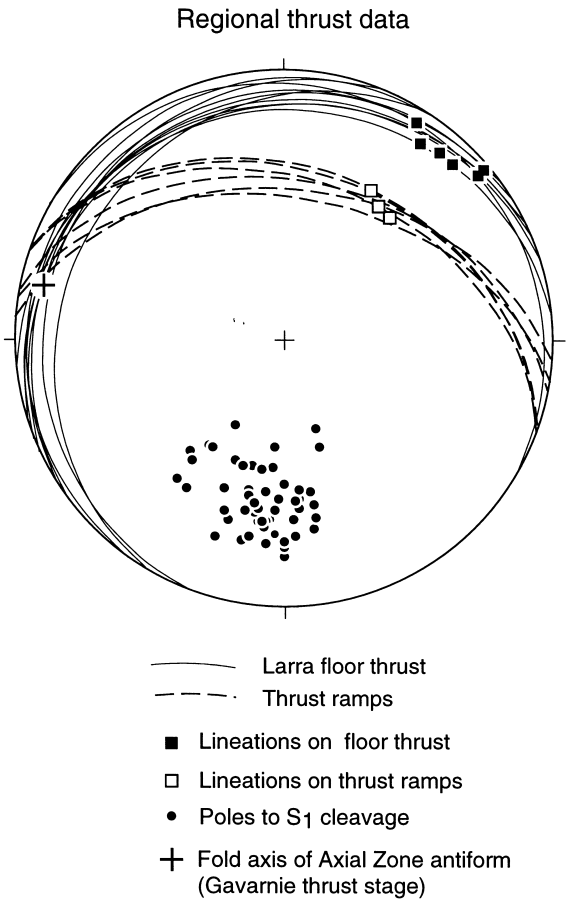

Fig. 6. Stereoplot of main structural elements of the Larra thrust system in the northern Axial Zone region. Cleavage poles are from the Zuriza shales and the impure limestone member.

it has been affected by homogeneous internal deformation (Fig. 4a). The Larra thrust dips parallel to footwall bedding, at gentle angles to the N or NNW, due to post-thrust tilting during the development of the Axial Zone antiform (Gavarnie thrust stage). Both the Larra thrust system and its footwall are cut by a late system of high-angle normal faults (Figs. 2 and 5) whose orientation ranges between WNW–ESE and NNE–SSW (Teixell, 1990; Hervouèt, 1997). These faults appear related to tangential longitudinal strain stretching over the Axial Zone antiform.

The internal ramps of the Larra thrust system strike WNW–ESE to NW–SE (Figs. 5–7). Most ramp surfaces dip approximately 25–35° relative to the floor thrust, and they are fairly regularly spaced (usually 200–300 m in the restored state). Thrust-related folds (hanging wall anticlines, e.g. Fig. 8) are present in association with some of the ramps; they are of metric–decametric scale and markedly asymmetric, with gently dipping backlimbs and vertical to overturned forelimbs.

Each of the Cretaceous stratigraphic units displays its own style of thrust-related deformation. The lower limestone unit, in the footwall of the décollement shows little other than homogeneous layer-parallel shortening, expressed by crude cleavage fissility (Durney and Kisch, 1994) in outcrop and flattened peloids and microfossils representing type 1 or grain cleavage (Durney and Kisch, 1994) in thin section (Fig. 4a). Rough slaty-type and spaced cleavages (Durney and Kisch, 1994), and an abundance of extension-veins as well as thrust ramps, are typical of the upper limestone unit. The cleavage at this level is somewhat inclined to bedding, suggesting a component of shear as well as layer-parallel shortening. The overlying Zuriza shales show a generalized slaty cleavage all over the region, and usually very little veining except near ramps. In the study area, this cleavage strikes E–ESE on average, dips moderately to steeply N (Fig. 6), and has a down-dip stretching lineation and a 'very strong' cleavage fissility (cleavage/bedding fissility ratio > 10 on the intensity scale of Durney and Kisch, 1994). The features of this unit indicate that it is the most ductile and least competent and has undergone significant shear deformation.

Minor structures developed in association with the ramps and folds provide interesting inferences for the kinematics of the Larra thrust system as a whole. They have been studied at two localities in particularly well-exposed road cuts: at Pierre-Saint-Martin (see location in Fig. 5) and at the Refugio de Belagua.

3.1. Ramp locality at Pierre-Saint-Martin (0°46′9″E, 42°58′16″N)

At this locality, a thrust ramp inclined some 40° to the north brings in contact the middle part of the impure, chert-bearing limestone member (unit B on Fig. 3) and the shaly upper part of this stratigraphic unit (Fig. 7). Stratigraphy in both fault walls is truncated in a ramp-over-ramp geometry. Cutoff angles are fairly similar in hanging wall and footwall (about 12°), and there are no folds. The attitudes of structural elements at the locality are plotted in Fig. 7. The fault zone is characterized by two main subparallel fracture surfaces, which enclose an intervening rock slice 1 m thick. This slice is strongly deformed and displays an internal oblique foliation coherent with ramp shear. The fault surfaces are slickensided, as are some of the foliation planes, suggesting late reactivation. Within the wall rocks, there are contractional, conjugate en-échelon arrays of calcite veins. As the shortening axes of the arrays have been tilted together with bedding, they indicate an early episode of layer-parallel shortening prior to folding. An incipient foliation, oblique to bedding, is also present (Fig. 7). Transport directions (contraction or shear), which can be deduced from the

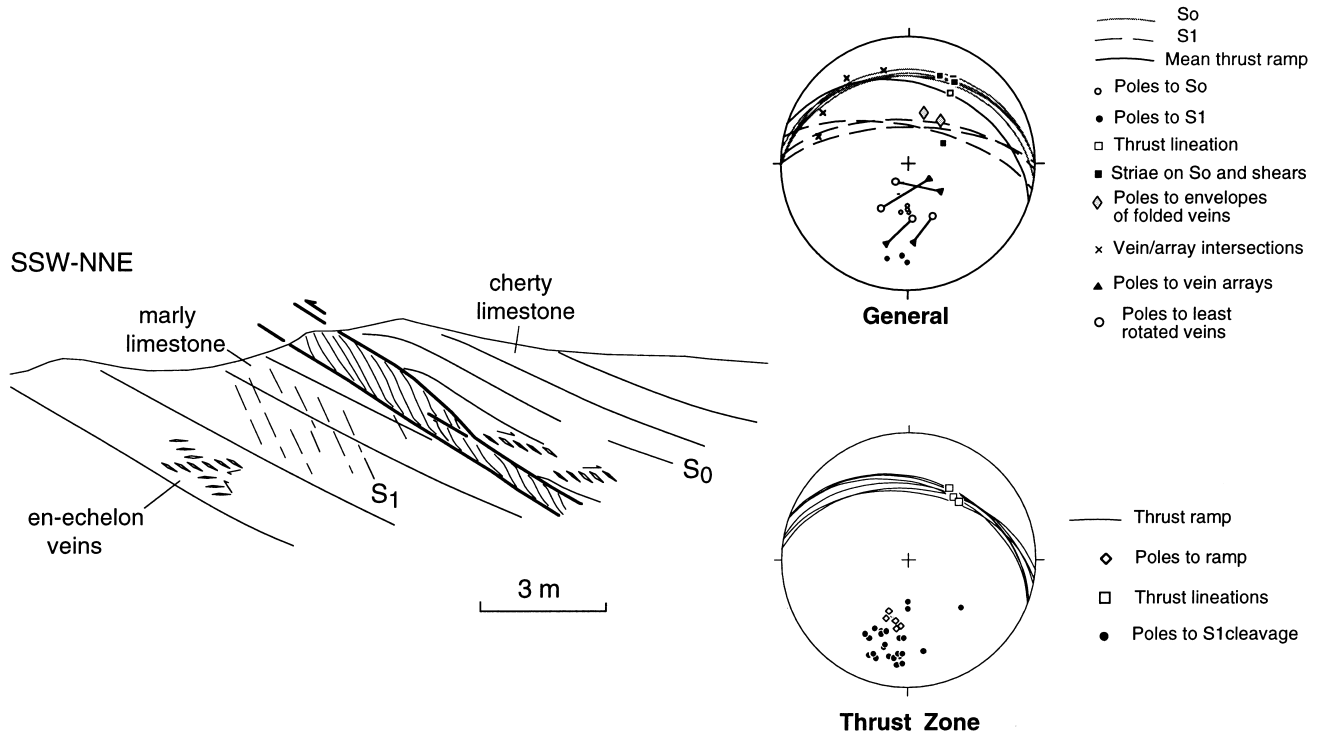

Fig. 7. Outcrop sketch and plots of minor structures of the ramp locality at Pierre-Saint-Martin (see location in Fig. 5). The regional (post-thrust) tilt of the Larra thrust system at this locality is gentle.

orientation of minor structures, range from N–S to NE–SW.

3.2. Ramp-fold locality at Refugio de Belagua (0°50′53″E, 42°56′36″N)

This locality is in the roadcut immediately below the Refugio militar de Belagua, 5 km to the southwest of the area mapped in Fig. 5. The bedded limestone unit defines an asymmetric, hanging wall anticline (Fig. 8). The thrust fault is poorly exposed on the southern slopes below the road, and brings the impure limestone member over the Zuriza shales. Structural elements of the locality are plotted in Fig. 8. The fold axis plunges 315/6, and there is an axial planar foliation, defined in the limestone by spaced solution seams or by more homogeneous intra-granular deformation features such as flattened foraminifera. As at the previous locality, there are early arrays of en-échelon veins. At this locality they are strained by the fold-related ductile deformation. Depending on their orientation, the veins are folded and thickened or flattened and thinned, but reconstruction of their original attitude with respect to bedding indicates early layer-parallel shortening. In

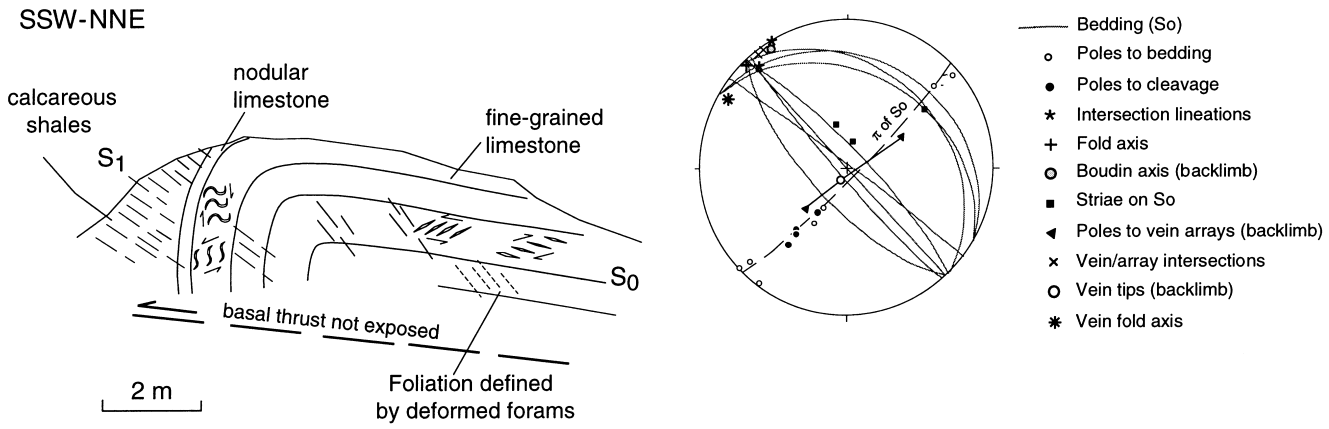

Fig. 8. Field sketch and plot of minor structures of the ramp fold at Refugio de Belagua, 5 km to the SW of Pierre-Saint-Martin.

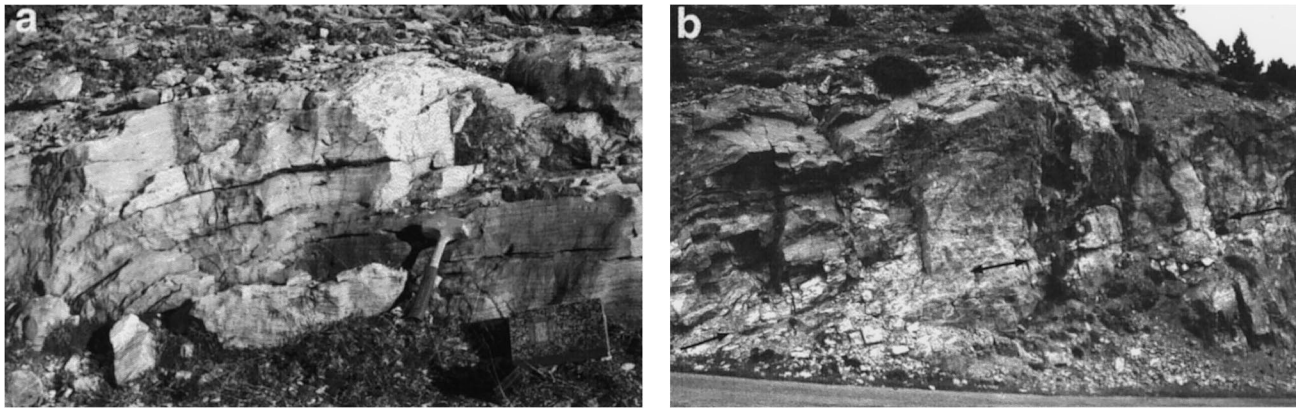

Fig. 9. (a) Typical aspect of the Larra décollement thrust in outcrop, with its characteristic white, foliated-looking fault-rock (photo taken by the road from Pierre-Saint-Martin to Arette). Hammer in the centre-right for scale. (b) General view of Pierre-Saint-Martin locality (location in Fig. 5, detailed profile in Fig. 11). Bedding in both hanging wall and footwall is parallel to the thrust. Arrows indicate the reference fault zone centre, a marked parting surface; the light-coloured band around the centre is caused by extreme concentration of calcite veins. View N 040 (thrust direction out of the page), roadcut is 6 m high.

spite of thrusting, this locality and similar ones elsewhere show a significant component of ductile strain during the Larra system evolution. Most of the minor structures (en-échelon arrays, fold axis, bedding-slip striations, cleavage, intersection lineations, and boudin axes) are consistent with a SW-directed tectonic transport (N 225 E) (Fig. 8).

4. Décollement zone structure

In the field, the Larra thrust appears as a metre-thick band of strongly foliated rock that, at first sight, resembles a mylonitic marble (Fig. 9a). However, closer inspection shows that its foliated aspect is due to a densely packed stack of bedding-parallel calcite veins.

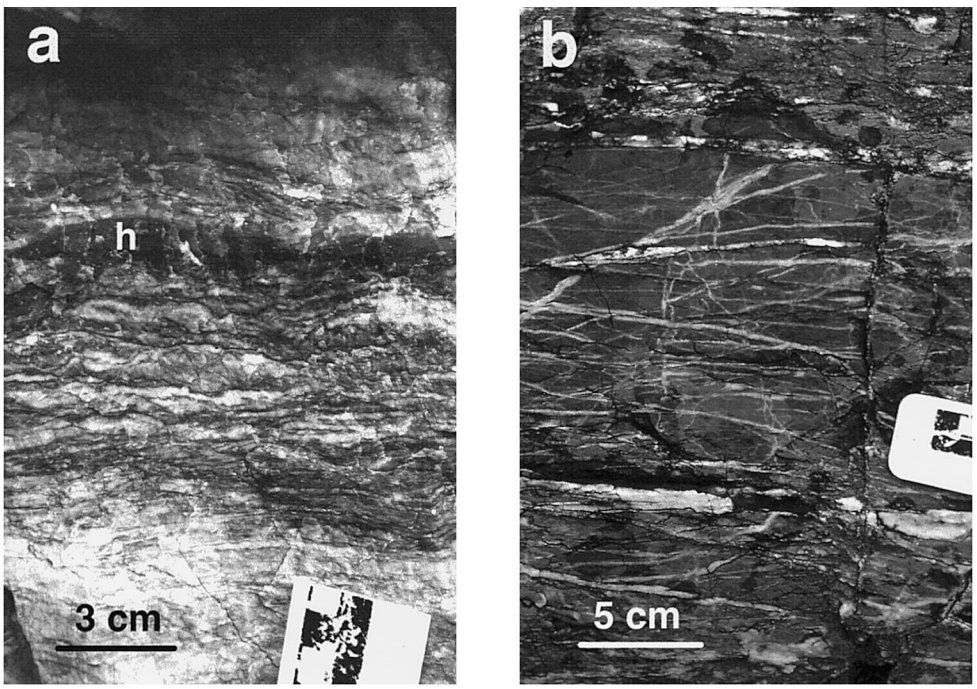

Fig. 10. Close-up field photographs of the Larra thrust fault zone (Pierre-Saint-Martin locality). (a) Dense veining at the fault zone centre, of dominantly parallel to bedding and to the thrust. Veins form almost 100% of the rock volume, with minor slivers of host limestone, labelled 'h'. Oblique stylolites (sloping gently and steeply right) and gentle folds are also present. View N 010. (b) View of damage zone 110–140 cm above the reference fault zone centre (view N 015). Horizontal veins correspond to the thrust-parallel A-vein set. Moderately W-dipping and high angle veins (M and N sets, respectively) are also visible.

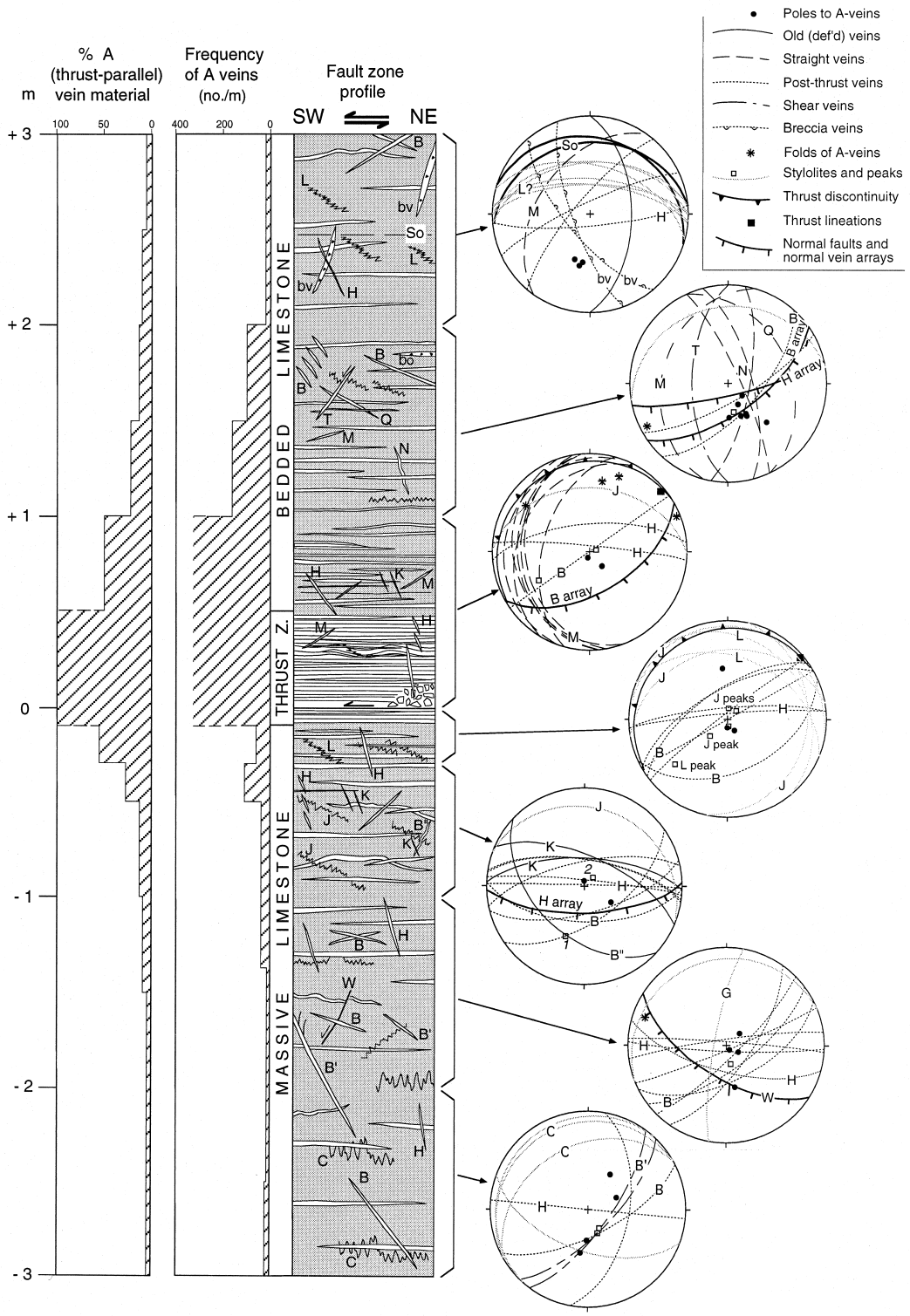

Fig. 11. Structural profile of the Larra décollement thrust fault zone and adjacent wall rocks at Pierre-Saint-Martin, measured normal to the fault plane relative to fault-zone centre (0 m), view N to WNW. Positions and observed cross-cutting relations of chief structures are shown. Thrust-parallel veins are labelled 'A'. Other letters refer to different sets of veins, stylolites and other minor structures, as indicated in the legend. Orientations are on the right; percentage and frequency of A veins on the left.

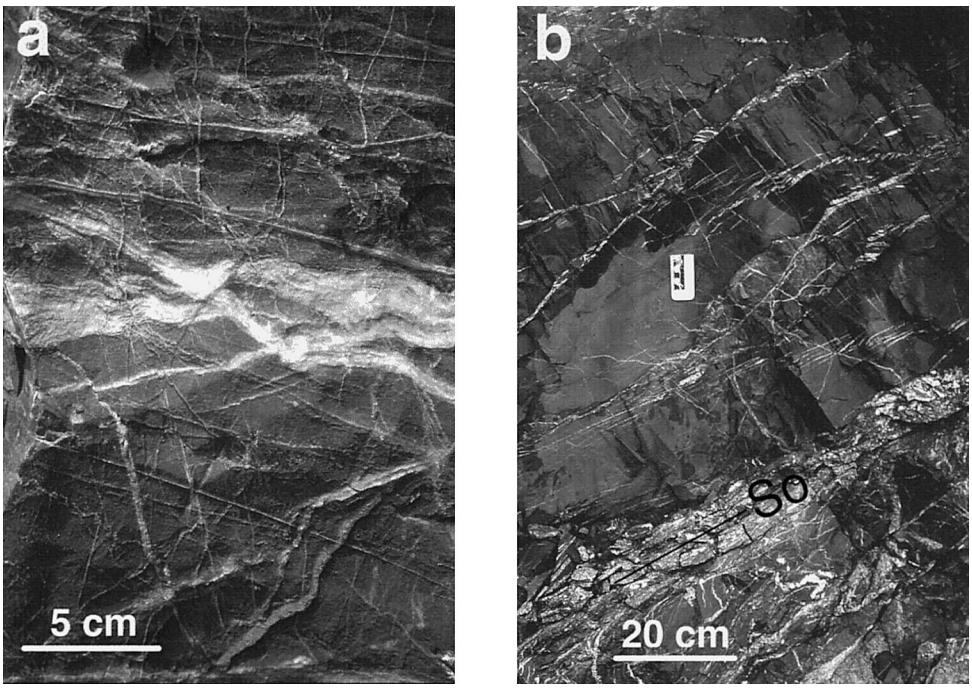

Fig. 12. (a) Multiple generations of A-veins (older and slightly buckled to thin and straight) and associated branching B″-veins (sloping left). Footwall limestone, Pierre-Saint-Martin locality, 0.7 below fault zone centre, view N 320. Steep post-thrust (H) veinlets are also present. (b) Hanging wall limestone some 16 m above the fault zone centre, showing en-échelon arrays of bedding-parallel A veins, view N 270, Pierre-Saint-Martin. Bedding is indicated as 'S_0'. The white zone through 'S_0' contains brecciated fragments of older vein material: a breccia vein.

Bedding-parallel veins are abundant for at least 3 m in both hanging wall and footwall, and their frequency increases towards the fault zone centre, where the rock appears formed by almost 100% vein material (Fig. 10a). Cross-veins, oblique to bedding, are also present, although less abundant (Fig. 10b).

A detailed profile of the décollement fault zone of a selected locality at Pierre-Saint-Martin (Fig. 9b), close to the French–Spanish border (0°46′5″E, 42°58′12″N) is presented in Fig. 11. Other outcrops in the northern Axial Zone show features similar to those at Pierre-Saint-Martin; therefore the chosen profile is believed to be representative of the Larra thrust in this region. There is a complex assemblage of diverse mesostructures that, apart from the veins include vein breccias, stylolites, folds and minor faults. On the basis of aspect, orientation and relationships to one another, the mesostructures have been correlated across the profile and grouped in sets. For identification purposes, arbitrary letters are assigned to each set (Fig. 11), according to order of observation up the profile.

4.1. Thrust-parallel veins

Bedding-parallel (and hence thrust-parallel) veins, labelled as A-veins (Fig. 11), are the dominant structures throughout the fault zone. The abundance and concentration of these veins in the fault zone, together with their consistency in orientation with regional sub-horizontal shortening, suggest they are genetically related to the thrusting process. There are several generations of these veins, giving evidence of formation over a long period of time. Older A-veins are folded and show little internal structure (Fig. 12a), suggesting they had undergone internal deformation and recrystallization. Younger A-veins are straighter, cemented by relatively clean crystals and cross-cut older ones (Figs. 12a and 13a). Like other veins in the limestone, A-veins are filled exclusively by calcite. Length of the veins commonly ranges from 5 cm to 2.5 m, and exceptionally up to several metres. Vein thickness lies most commonly between 1 and 3 mm, although numerous very thin ones (up to 20 μm), and fewer thicker ones ($\geq$1 cm) have also been observed. The frequency of mesoscopically distinct A-veins and the proportion of these veins to the total rock, as counted over sub-metric intervals, increase exponentially towards the fault zone centre, where they are extremely concentrated in a 60 cm-thick central band (histograms in Fig. 11). They tend to be more abundant and persistent in the hanging wall than in the footwall. A faint lineation (N45–N50) is locally observed on the surfaces of veins in the fault zone, expressed as a weak ribbing. This is interpreted as a slip lineation, though it is unlike slickensides or striations in appearance (which have nowhere been observed on these veins). Laminated slip-fibre structure, as in the shear veins described by Cox (1987),

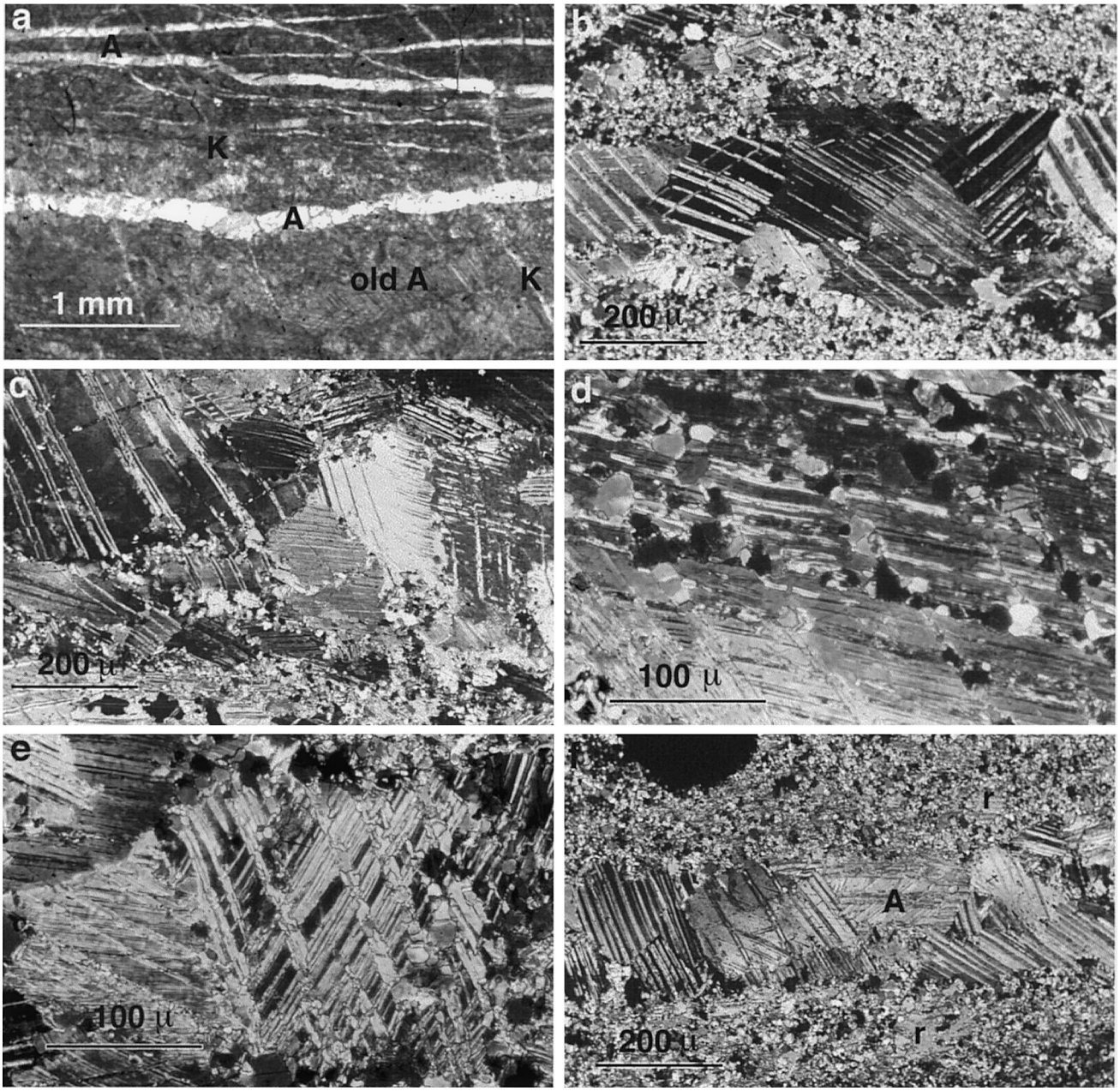

Fig. 13. Photomicrographs of fault-rock from the fault zone centre. Sense of shear is top-to-left in all images. (a) Plane-polarized light aspect of thrust-parallel (A) veins and high angle veins. Younger, cleaner A-veins cut older, darker ones (old A). (b) Thrust-parallel vein cemented by blocky calcite crystals. Some crystals display planar, subidiomorphic faces. All exhibit strong twinning. Crossed polars (XPL). (c) Detail of a thrust-parallel vein showing rotation recrystallization (core and mantle texture) at crystal boundaries. XPL. (d) New recrystallized grains along twin lamellae in a vein-calcite crystal. XPL. (e) Twinned crystals showing evidence of twin boundary migration. XPL. (f) Young A-vein with little internal recrystallization cutting a recrystallized aggregate derived of former A-vein material. Relics of the original crystals of the earlier veins, 'r', can still be observed.

Labaume et al. (1991), De Roo and Weber (1992), etc., is likewise absent. Brecciation of both vein and wall-rock material may, however, be present.

4.2. Other structures

In addition to thrust-parallel veins, there are various sets of oblique veins and other structures, indicating a complex deformational history. The structural column in Fig. 11 shows the more prominent representatives of these structures and their cross-cutting relationships, based on outcrop sketches and photos in the profile section. Attitudes are shown in the accompanying stereoplots. Bedding-parallel stylolites C, with up to decimetric (10-cm-scale) peaks, are the earliest features to be formed, and may be attributed to sediment com-

paction prior to tectonic deformation. They are more abundant in the footwall limestone than in the hanging wall. Some of the veins and stylolites that are oblique to the thrust plane (e.g. veins B″, K, M, N, Q, stylolites J and L, Fig. 11) show cross-cutting relationships indicating formation that alternates with the thrust-parallel veins, and hence simultaneous with thrusting. Veins B″ which dip to the SW and appear folded (Fig. 12a), are amongst the oldest oblique veins and occur only in the footwall, whereas veins M (Fig. 10b), N (Fig. 10b), and Q, which dip W and E, oblique to the regional transport direction, are characteristic of the hanging wall. Small, NNE-dipping K-veins are common in both the hanging wall adjacent to the fault zone and in the footwall. Gently N- to E-dipping stylolites J (with steep peaks) and L (later, with subhorizontal peaks) (Fig. 10a) are roughly consistent with regional shear and are equally distributed across the profile. All of these structures are cross-cut by late, undeformed A-veins, which in turn are cut by steep, diversely oriented, hanging wall breccia veins (bv).

Minor normal faults (W), steep extension-veins (F, H, B) in sinistral-sense en échelon arrays, and dextral-sense shear-veins (B′) cross-cut all of the previously mentioned structures (e.g. thin H-veins in Figs. 12a and b). They are correlated with the post-thrust extensional fault system of the Axial Zone culmination (Gavarnie stage). These are present in both hanging wall and footwall, and always cut veins A and other thrust-related structures. Vertical dissolution may accompany these structures, causing reactivation and small sub-vertical peaks on some earlier C-, J- and L-stylolites, especially in the neighbourhood of normal vein-arrays. The attitudes are shown in the stereoplots accompanying Fig. 11 ('post-thrust veins' and 'normal faults'), and will not be discussed further.

4.3. Summary of thrust-related kinematics

Rather than enter into details of the structural history (which are complex), we summarize here the kinematic and mechanical aspects of mesostructural observations that seem most relevant to a consideration of the thrust mechanics.

1. Thrust-parallel A-veins and breccia veins are the earliest recorded tectonic structures and the most persistent in time. They are also the most widespread structures, especially in the fault zone, and attest to predominant brittle behaviour of the décollement. The nature of these veins is discussed further in the microstructural and model sections, below. They appear to have originated as extension-fractures in a regime of subhorizontal compressive stress (en échelon arrays are widespread in the hanging wall: Figs. 7, 8 and 12b). The thrust-parallel breccia veins (Fig. 12b) contain disrupted crystalline material that is best explained by brittle shear displacement of partial infills and earlier vein deposits in the walls and bridges of preexisting extension-fractures. Thus, although there is little direct evidence for shear displacement on them, these structures and deformed A-veins of the fault zone centre (Fig. 10a) are the ones most likely to have carried the thrust movement.
2. Stylolites J and L show multiple relations to veins, suggesting development over relatively long periods and, together with recrystallization, modified the vein structure of the fault zone. They are spatially most closely associated with A-veins (Fig. 11), but show some layer-parallel shear strain (stylolite surfaces at moderate or low dips and steep peaks on J-stylolites) as well as layer-parallel shortening kinematically consistent with the A-veins (subhorizontal peaks on L-stylolites). Thus they can be considered to represent periods of accumulating but moderate ductile contractional shear which alternated with mainly contractional brittle deformation. Incremental transport directions, inferred from asymmetry of surfaces and directions of stylolite peaks, range between S and WSW, as do the kinematic axes of en échelon A-veins.
3. B″ and M veins are extension-veins that lie oblique to the thrust plane, consistent with SW- to W-directed horizontal shear. N-veins, which are steeper and slightly buckled, probably originated in a similar way but were shortened and rotated by continued shear.
4. The other syn-thrust veins mentioned above (K, P and bv) cannot be directly related to forelandward shear or contraction as they dip too steeply, or in the wrong direction, and have not been buckled. Speculative origins for these structures could include (a) dynamic reverse shear due to rebound during seismic slip, (b) layer-parallel extension at the trailing end of slipped hanging wall segment and (c) bending of the hanging wall during transport over décollement irregularities (cf. cataclastic seams of Wibberley, 1997, analogous to 'bv' breccia veins in this study).

4.4. Vein microstructure

Calcite crystals within all veins show coarse (sparry) blocky textures (Fig. 13). Crystal sizes commonly vary between 400 and 600 μm for the thickest veins, and from 100 to 200 μm in thin ones. Some veins show a first generation of rim cement in the form of small idiomorphic crystals. Frequently, crystals in veins are tabular, parallel to the vein walls; in thick veins they

can reach a length up to 6 mm. Neither fibres nor host-inclusion trails have been observed, and crack–seal microstructure is lacking. It appears that each of the veins formed by a single event of dilatant fracture opening, followed by cementation. Based on vein widths, dilation apertures (commonly millimetric dimensions) were generally greater than those associated with crack-seal (ca. 100 μm, Ramsay and Huber, 1987).

Twinning is a widespread internal deformation mechanism in calcite crystals, not only within veins but also in echinoderm ossicles in wall rocks, even several metres away from the décollement zone. Twin development is related to grain size; twins are rare or absent in small crystals forming the carbonate cement of grainstones and in very thin veins, but they are extremely abundant in medium to thick veins. Twin thicknesses typically vary from 5 to 10 μm, a value that appears more dependent on grain size than on position within the fault zone profile.

Whereas all crystals in thrust-parallel (A) veins from the central zone of the fault contain deformation twins, sometimes bent, there is a variable degree of recrystallization. Youngest, usually small veins show twins with sharp boundaries (Figs. 13b and f) and minor evidence of twin-boundary migration. Older, usually thicker veins display small recrystallized grains at crystal boundaries (core and mantle texture) or at twin lamellae (Figs. 13c and d), and more evidence of both twin-boundary and grain-boundary migration (Fig. 13e). In addition, twins show unconstricted ends. Rotation recrystallization may have progressed to replace wider regions or entire crystals, producing mosaics of equiaxed grains of individual size ca. 8–10 μm. These grains appear strain free at the optical scale. At advanced stages, the entire vein may be transformed into a fine-grained aggregate of new grains, whose former origin may only be recognized by patches of crystals of comparable crystallographic orientation, i.e. remains of parent grains (Fig. 13f). In some cases, it may be difficult to distinguish the recrystallized vein material from the host-rock, although the latter shows a slightly smaller grain size (about 5 μm). Poor recrystallization in twinned crystals far from the fault zone centre indicates that there is not a unique correlation between recrystallized twin appearance and temperature (e.g. Burkhard, 1993). Instead the twin aspect here is a function of proximity to the thrust plane and therefore an effect of strain.

Although twinning was the dominant deformation mechanism in the large vein crystals, intracrystalline slip systems were also active, with a certain amount of dislocation creep. Dislocations piled at twin boundaries, and temperature was enough to induce efficient recovery and recrystallization there, as well as in stressed grain boundaries. However, the original or relict crystals do not appear to be much elongated, as the microstructural development was dominated by grain-size reduction. Neither are the new grains in recrystallized aggregates elongate. Hence, it is to be remarked that grain-shape fabric does not contribute to the rock's foliation, which is mainly defined by the vein concentration or by grain-size variations related to recrystallization. Kinematic indicators at the microscopic scale also have not been observed. Oblique veins show less evidence of recrystallization, although early ones also show various twin sets. When they are hosted by an earlier recrystallized aggregate, vein boundaries are diffuse or scalloped, attesting to grain boundary migration between host and vein crystals (Fig. 13f). Late oblique veins (post-thrust stage), which cross-cut all thrust-parallel veins, may exhibit twin-free crystals.

In spite of their different mechanical significance, veining and ductile deformation occurred in a progressive way during the same epoch. Little-recrystallized veins cross-cut older ones with more advanced recrystallization (Fig. 13f), suggesting cyclic concurrence of brittle and ductile behaviour during deformation. Interestingly enough, slivers of limestone host-rock between veins keep the original fine-grained micritic or microsparitic texture, and do not show much deformation; original carbonate components, such as peloids or echinoderm plates, may still be recognized. Intracrystalline deformation was partitioned and concentrated in the coarser-grained vein material, possibly at times of peak stress during fracturing, while the material was in a transitional brittle–ductile state. Repeated cycles of deformation, fracturing and infilling explain why older veins experienced progressively more deformation and recrystallization than younger veins. Solution-transfer activity complemented this process by providing a source of material to fill the fractures, most probably by diffusion from the stylolites in fine-grained protolith and recrystallized material. On the other hand, the apparently low finite strain and lack of shear indicators argue against ductile deformation being a major contribution to thrust displacement. Either ductile slip occurred in ways that left no clear imprint, or displacement occurred during loss of cohesion at times of brittle failure.

5. Mechanical model of décollement

In this section, we discuss the material properties and environmental conditions that may have influenced the development of a décollement in limestone, then we outline a mechanical model which accounts for the particular features and problems of the Larra thrust. Questions that are addressed include: What were the stress and fluid-pressure conditions at the

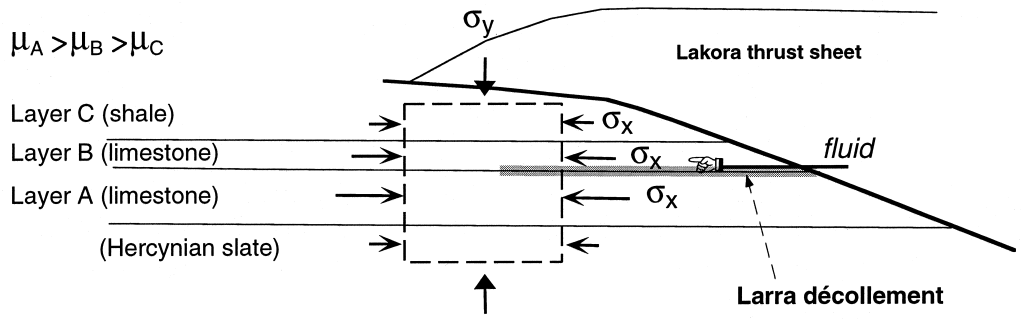

Fig. 14. General tectonic and mechanical setting during development of the Larra thrust, in the footwall of the Lakora thrust, a major Eocene convergence zone in the Pyrenees (not to scale). The Cretaceous limestones are more competent than the underlying Paleozoic basement and overlying shales and turbidites, and channelled horizontal stress (σ_x). Layers A, B and C are the mechanic lithic units referred to in Fig. 3 and in the décollement model (Fig. 18).

time of thrusting? Why does the décollement occur in the limestone? How does shear stress develop (which is necessary for fault slip) from initial conditions of layer-parallel principal stress (as indicated by the veins)? What determines whether the décollement propagates or the hanging wall undergoes imbrication?

5.1. Strength of layered units

Arguments which suggest that the Cenomanian–Santonian limestone was a strong lithologic unit at the time of thrusting, compared with the basement slates and overlying shales and turbidites, are: (a) cleavage is weaker and at a higher angle to bedding in the limestones than in the shales and turbidites, (b) limestones in other fold-and-thrust belts are known to have greater ductile competence than shales and slates, as shown by fold-thickness characteristics (Durney, 1972a; Ramsay, 1981; Julivert and Arboleya, 1984; Pfiffner, 1993) and twin-strain axes (Ferrill and Groshong, 1993), and (c) laboratory tests typically show limestone as having greater brittle strength and elastic stiffness than shales, slates and greywackes (Deere, 1968; Jaeger and Cook, 1969). This supports the view that primary mechanical weakness was not responsible for localizing the décollement.

5.2. Stresses

The prevailing thrust-tectonic regime that existed in this area (see structures in Figs. 2 and 5) implies that the regional maximum and minimum compressive stresses were subhorizontal and subvertical, respectively. In fact, bedding-parallel shortening indicators are a prominent characteristic of this thrust system, especially in the limestones: bedding-parallel A-type veins and L-type stylolite peaks, steep cleavage, low-angle vein-arrays and thrust-ramps. Therefore the axes of maximum principal stress (σ_1) and maximum shortening (e_1) must have been parallel to or at a low angle to bedding for much of the time during thrusting. As bedding-parallel extension-veins and breccia-veins are the oldest recorded tectonic structures associated with the Larra thrust and occur repeatedly throughout the movement history, we infer that σ_1 was layer-parallel both before the onset of thrusting and between subsequent slip increments. (This, of course, poses the problem of how the slip occurred, a point that is addressed in our model.)

Prior to slip on the décollement, the layers would have been stuck to each other and therefore subject to approximately uniform layer-parallel shortening strain rate ($\dot{e}_x$). Under this condition, the relation

$$\sigma_x - \sigma_y = 4\mu\dot{e}_x \quad (1)$$

(Treagus, 1973, eq. 3) shows that differential stress ($\sigma_x - \sigma_y$) varies between the layers in proportion to layer viscosity (μ). Differential stress would thus have been concentrated or 'channelled' in the competent limestone compared with the less competent basement slates and overlying shales (Fig. 14). Consistent with this prediction, several observations indicate relatively high differential stress in the limestone: (a) twins in vein-calcite, (b) straight vein tips (Thomas and Pollard, 1993), (c) competition between brittle and ductile deformation (conditions close to the strength limit) and (d) thrust-ramps (a high stress, shear mode of brittle failure). Such stresses had evidently made the limestone susceptible to brittle deformation, which is believed to be the chief reason why the thrust was located in that unit.

5.3. Fluid pressure

Abnormally high fluid pressure can also assist overthrust faulting (Hubbert and Rubey, 1959), both by lowering friction and by reducing shear strength of the fault plane. As the top of the stratigraphical succession consists of low-permeability shales and turbidites, fluids are likely to have developed abnormally high

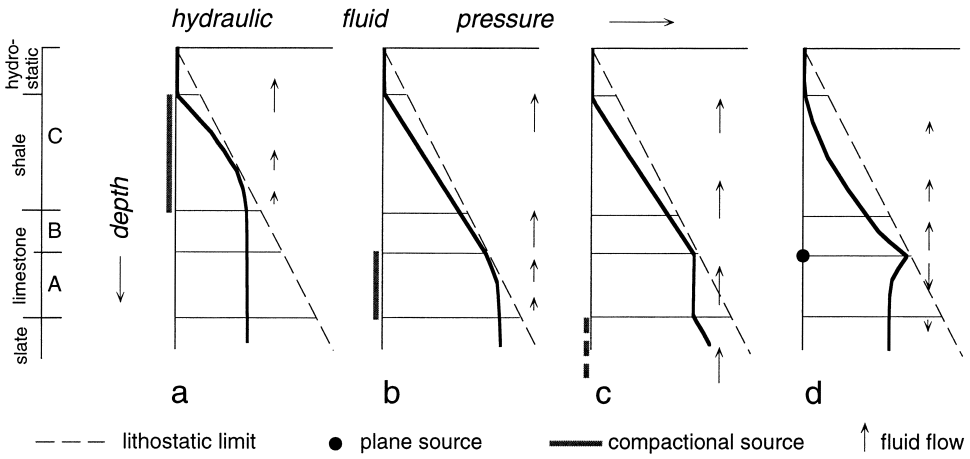

Fig. 15. Schematic hydraulic fluid-pressure/depth curves for different fluid-input scenarios in the layered sequence of Fig. 14. (a) Fluid generation from shale unit (layer C). (b) Fluid generation from lower limestone unit (layer A). (c) Uniform upward flow in layers of varying permeability (J.C. Moore, personal communication, 1999). (d) Hinterland input from active (Larra) thrust.

pressures at lower levels. Four possible sources of fluid and their associated hydraulic pressure gradients are shown schematically in Fig. 15. 'Hydraulic pressure' means the excess of fluid pressure over normal hydrostatic pressure and is the pressure that governs flow of the fluid. Décollement is most likely to occur where the hydraulic pressure curve is closest to the lithostatic limit (lithostatic pressure less normal hydrostatic pressure). The layers in Fig. 15 are labelled as in Figs. 3 and 14. The basal slate and layers B and C, which are clay-bearing, are assigned low permeabilities, except for the top of layer C which is considered to be open to surface waters. Layers A and C are potential distributed sources of fluid generated by horizontal compaction during layer-parallel shortening. These sources develop convex hydraulic profiles, such as shown in Fig. 15(a) and (b) (cf. Bolton, 1979). If fluid is sourced from below layer A limestone and if this limestone is permeable, by Darcy's law the hydraulic gradient in layer A will be flat whereas the gradients in less permeable units above and below will be steep (Fig. 15c). Fig. 15(d) shows a source of fluid at higher pressure than the surroundings. The fluid is channelled along a permeable horizon (the developing Larra thrust) in otherwise low-permeability rock, analogous to décollement zones in fine-grained sediments of modern accretionary prisms (e.g. Moore, 1989). In this case, the fluid is generated by episodic pumping in the rear, either from the Lakora thrust sheet (Fig. 14) or by hinterland segments of the fault itself.

It is immediately apparent from Fig. 15 that scenario (a) cannot produce the necessary high fluid-pressure at the observed level of the décollement (the junction between layers A and B). Instead, this case would produce a décollement somewhere within the impermeable part of layer C.

The other scenarios could all produce high fluid-pressure at the B/A junction. An argument for scenarios (b) and (c) is that the impermeable layers B and C could have prevented layer A from being fully dewatered during burial, so that layer A would have possessed the porosity or permeability, respectively, necessary for these models at the onset of thrusting. However, well-developed horizontal (C-type) stylolites and probable associated cementation in layer A limestone suggest that compaction was already well advanced, if not complete, by the end of pre-thrust burial. In scenario (c) there is also doubt about whether the previously metamorphosed basement slate would have been an adequate source of fluid for that model.

In contrast, scenario (d) (Fig. 15) requires that layer A and layer B were both impermeable at the onset of thrusting, which is supported by the pre-thrust C-stylolitization of these layers. The observed dense veining in the Larra thrust zone and the high time-averaged fracture permeability that this implies are also consistent with the thrust being a major passageway for fluid. However, scenario (d) does not in itself explain why the décollement was located at the B/A contact. Also, fluid pressure alone does not seem to account for the detailed distribution of brittle deformation around the thrust plane. In model (d) it should be symmetrical above and below the thrust, and in models (b) and (c) we expect that it would be strongest where the high fluid-pressure is generated: near the top of the footwall. Instead, fracturing is stronger in the base of the hanging wall (Fig. 11) and thrust-ramps occur only in the hanging wall. These points are addressed in our mechanical model. But, first, it is necessary to examine the critical question of vein dynamics and modes of brittle failure.

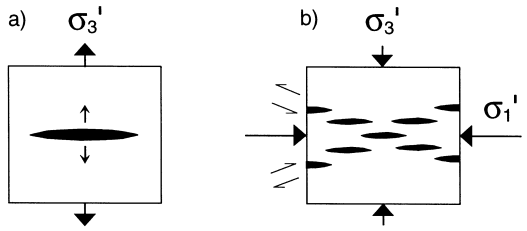

Fig. 16. Models for formation of extension fractures. (a) Tension (hydraulic fracture) model: σ_3', the least effective stress (least stress, σ_3, minus pore fluid pressure, p), is tensile; rock fails by unstable propagation of a single macroscopic extension crack. (b) Compression model: σ_3' is zero to moderately compressive; σ_1', the greatest effective stress, is large and compressive; crack-propagation is stable and rock fails by macroscopic shear along en-échelon crack-arrays.

5.4. Fracture models and origin of veins

Hydraulic fracturing (Fig. 16a) is often invoked to explain horizontal veins in compressional terrains (Secor, 1965; Phillips, 1972; Etheridge, 1983; Sibson, 1989; Henderson et al., 1990; Cosgrove, 1993, etc.). It assumes that the rock fails in effective tension ($\sigma_3 - p = -\sigma_t$): i.e. when fluid pressure (p) exceeds the overburden pressure (σ_3) by an amount equal to the tensile strength of the rock (σ_t). This requires extremely high fluid-pressure and relatively low differential stress ($0 \leq \sigma_1 - \sigma_3 \leq 4\sigma_t$), conditions that seem most likely to be met in strata of high water-generating capacity, low permeability and low tensile strength subject to weak tectonic compression. Each failure event produces only one runaway extension crack, so that multiple cracks require repeated failures and multiple regeneration of the high-pressure fluid.

Contrasting with this is what we call the 'compression model' for extension fracturing (Fig. 16b), whose effects have been widely reported in uniaxial and triaxial compressive strength tests of brittle rocks. Fig. 17 summarizes the behaviour observed in such tests by Gramberg (1965), Brace et al. (1966), Wawersik and Fairhurst (1970), Wawersik and Brace (1971), Hallbauer et al. (1973), Tapponnier and Brace (1976) and Wong (1982). The mechanical regions are those of Brace et al. (1966), as modified by Paterson (1978). Points of interest are:

1. Extension cracks nucleate and grow under both zero (uniaxial) and compressive (triaxial) effective confining pressure: i.e. $p \leq \sigma_3$ rather than $p > \sigma_3$.
2. Close to peak stress (top of region III), the cracks concentrate in inclined zones of incipient shear or en échelon arrays (e.g. Gramberg, 1965, fig. 8, for limestone and Wawersik and Fairhurst, 1970, fig. 5, and Olsson and Peng, 1976, fig. 6, for marble).
3. The crack-arrays collapse to form shear-failure planes or faults (region IV).
4. Applied differential stresses during extension-crack development approach the compressive strength of the rock (peak stress in Fig. 17) rather than the tensile strength: i.e. $\sigma_1 - \sigma_3 \geq 8\sigma_t$ rather than $\sigma_1 - \sigma_3 \leq 4\sigma_t$, using the plane Griffith criterion (Jaeger and Cook, 1969).

Extension fractures formed in this way thus develop in en échelon arrays rather than as single cracks, and

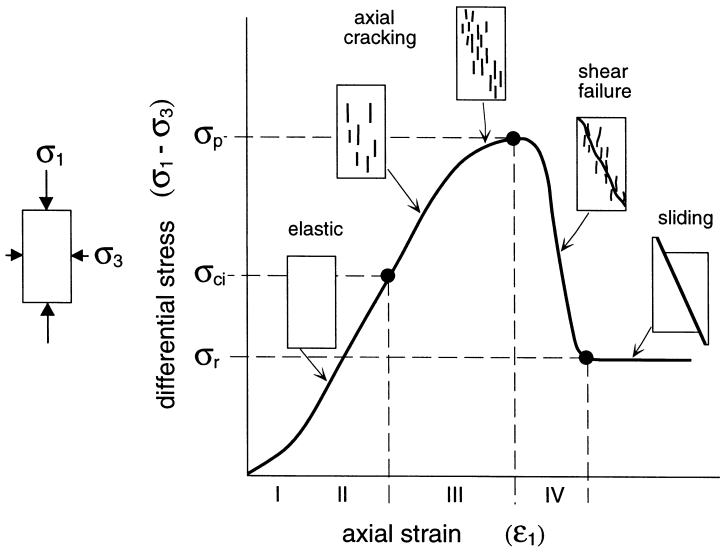

Fig. 17. Mechanical behaviour of brittle and semibrittle rock in low confining-pressure, triaxial compression experiments (summarized from observations of Brace et al., 1966, and others, see text for explanation). *Stages I and II:* elastic deformation. *Stage III:* initiation and growth of axial extension cracks, ultimately concentrating in inclined zones. *Stage IV:* shear failure by progressive collapse of a crack-array. *Post-Failure Stage:* frictional sliding on shear fracture. ($\sigma_1 - \sigma_3$: differential stress. ε_1: shortening strain. σ_p: peak strength of intact rock. σ_{ci}: crack-initiation stress. σ_r: residual strength of sheared rock.)

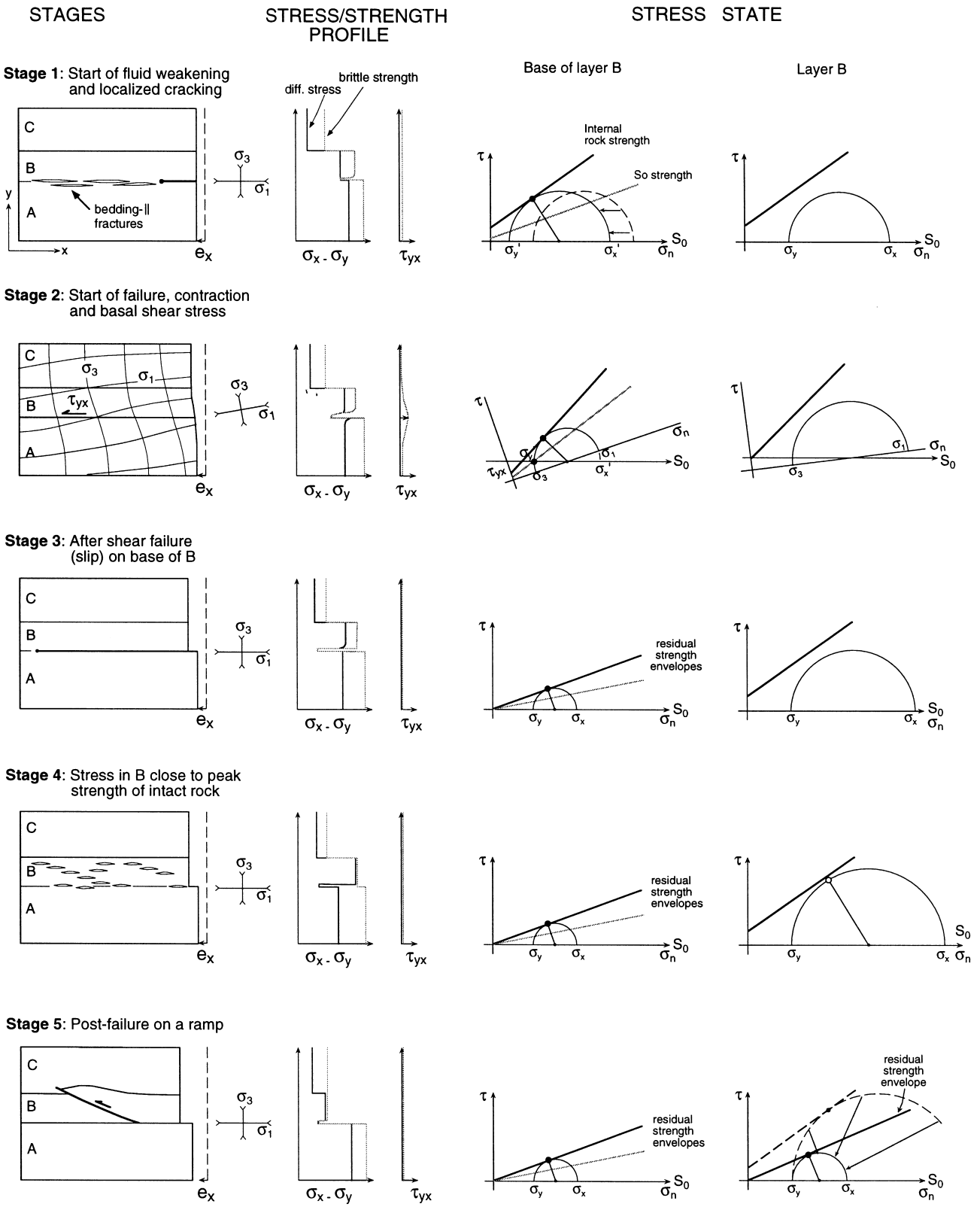

Fig. 18. A mechanical model for the development of the Larra décollement thrust (see text for explanation). Layers A, B and C correspond to strata in Fig. 3. (Layer A does not bear any relation to A-veins.)

are associated with shear fractures. These facts accord with the observed geometry of subhorizontal, A-type, extension veins associated with the Larra thrust. The compression model also better explains the occurrence of these veins in competent and possibly dewatered rock, the high density of the veins (multiple rather than single cracks), the development of fracture porosity (through linked extension cracks and shears) and the supply of vein-infilling material through local solution-transfer (linked stylolites and veins) which also depends on differential stress (Durney, 1972b).

The inference from the veins, then, is that differential stress in the limestone was high in relation to the compressive strength of the rock, and fluid pressure was probably equal to or less than overburden pressure. This agrees with indicators of high stress in the limestone discussed earlier, and suggests that differential stress was the primary influence on failure mode. Fluid pressure nevertheless affects the strength and frictional behaviour of the rock and so would have exerted a control on brittle deformation and slip on the décollement.

5.5. Décollement localization and propagation model

To account for localization of the décollement and propagation of shear displacement, we propose cyclical changes of stress related to differences in mechanical properties of the layers, prompted by periodic input of fluid at the décollement surface (scenario 'd' of Fig. 15).

Stage 0. The assumed initial or background state is where the layers A, B and C (see above) are firmly welded to one another and are undergoing steady ductile flow. This occurs either in unfaulted strata ahead of the décollement or in strata that have previously slipped, rehealed and re-equilibrated after an extended period of time. Differential stress $(\sigma_x - \sigma_y)$ at this stage varies in proportion to the viscosities of the layers and the major principal stress (σ_1) is subparallel to the layers, as discussed in Section 5.2. Background layer-parallel shear stress (τ_{yx}) is thus low and so we disregard this component in the model. Although differential stress in the limestone is high, it is presently below the level required for brittle failure. For the same reason, ambient fluid pressure must be below its maximum possible value (which we take to be the overburden pressure).

The analysis that follows considers mainly the elastic, plastic and brittle strains because of their particular relationships to changing stress associated with faulting. We assume that elastic moduli and brittle shear and compressive strengths reflect relative competencies of the layers roughly similar to viscosity. We also note that limestone B, which is finer grained and slightly arenaceous, will be somewhat less competent than limestone A. The conditions at each stage are shown in Fig. 18 as profiles of elastic strain, stresses and compressive strength. Conditions at Stage 0 are similar to Stage 1 (Fig. 18) except that brittle strength in layer B is uniform down to the base of the layer.

Stage 1. Stage 1 represents the beginning of fluid-assisted yield ahead of an active segment or tip of the décollement. The limestone layers at this stage, already under high stress, are susceptible to weakening by fluids. When fluid in the previously slipped segment of the fault (scenario 'd' in Fig. 15) reaches the end of the fault, its pressure rises there, causing a reduction of brittle strength and incipient brittle failure (yield, or middle of region III, Fig. 17) ahead of the displaced segment. (Alternatively, fluid pressure might rise due to compaction of the footwall limestone: Fig. 15b.) Yield occurs as a zone of randomly overlapping bedding-parallel extension fractures around the undisplaced contact. As the cracks are filled with water, they could be regarded as small water sills (cf. N. J. Price in Fyfe et al., 1978, but without implied genesis).

Stage 2. The cracks produced in Stage 1 allow further access to the external high-pressure fluid source, which results in fluid pressure rising towards lithostatic values, accompanied by further reduction of strength and differential stress there (i.e. reduced peak stress conditions). At the same time, strain increases due to further fracturing and elastic and plastic distortion of rock bridges between the cracks. However, the contact zone is not free to develop into a shear oblique to bedding, because of constraint by strong intact rock above and below. So behaviour at this point departs from the simple conditions of Fig. 17, as outlined below. At this stage, the contact zone still has some cohesion and can therefore support a shear stress.

The localized strain-softening noted above begins to allow relative movement between layers A and B, with consequent redistribution of the stresses within those layers. Now, it can be shown that the fully welded layer stack (Stages 0 and 1) is a minimum internal elastic strain-energy state when the strain is uniaxial in x and when total x-force on the stack is constant. This is a metastable state that will tend to change to one governed by maximization of work on the stack by the environment when layers become uncoupled. The change involves a transfer of horizontal force either from footwall to hanging wall across a decoupled contact or vice versa, and at present we have no definite criterion to determine which of these will occur. Intuitively, we think the horizontal force is more likely to be transferred from the more highly stressed footwall layer A to the less stressed hanging wall layers B plus C. If that is the case, then horizontal stress and elastic strain will rise in layers B and C and will fall somewhat in layer A and in the underlying basement.

These changes in horizontal stress imply a hinter-

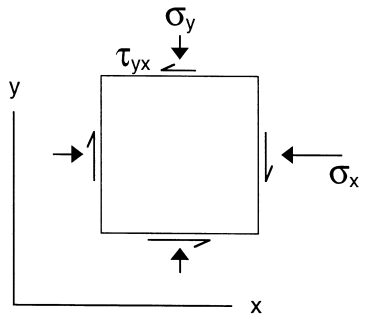

Fig. 19. Qualitative relation between vertical variation of shear stress (τ_{yx}) and horizontal variation of horizontal compressive stress (σ_x). Vertical stress σ_y is non-hydrostatic and considered constant.

land-increasing σ_x in layer B and a hinterland-decreasing σ_x in layer A. According to the condition for static equilibrium of stresses

$$\delta\sigma_x/\delta x + \delta\tau_{yx}/\delta y = 0 \quad (2)$$

(two dimensions and no body forces, after Ramsay, 1967, eq. 2-53, Jaeger and Cook, 1969, eqs. 5.5.5-7), this requires a downward-increasing shear stress τ_{yx} in layer B (Fig. 19) and an upward-increasing τ_{yx} in layer A. Hence a shear stress maximum occurs precisely at the B/A contact (Fig. 18, Stage 2). (This situation can also be argued in terms of elastic strain; the difference in horizontal strain, e_x, between the layers causes a shear strain around the B/A contact. In some respects it resembles a mode II or shear dislocation, but it differs from those models in not being driven by external shear stress.)

This effect accounts for the origin of the shear stress, which is necessary for décollement slip. The shear stress, and thus the continued localization of décollement at this level, is a result of differential strain between the hanging wall and footwall. In effect, the hanging wall peels off from the footwall at a competency step in the limestone, prompted by embrittlement of the limestone by high differential stress and fluid pressure.

Stage 3. Having been pervaded previously by bedding-parallel extension cracks, the contact zone is weakest in the plane of bedding and is thus susceptible to bedding-parallel shear failure. The shear stress that developed in Stage 2 may overcome this strength and initiate an increment of slip at that site. Failure is envisaged as occurring by rupture of the remaining rock bridges between the cracks (Fig. 20), probably accompanied by local plastic strain (Frederich and Evans, 1989), brecciation and foreland-dipping extension fractures. Displacement then occurs by rolling on breccia fragments, frictional sliding and glide on zero shear-strength water sills, which would explain the paucity of mesostructural record of the displacement.

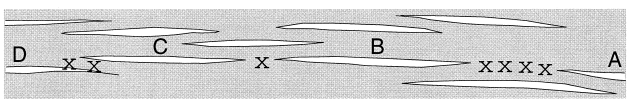

Fig. 20. Main mechanism of movement along the Larra thrust. Open, en-échelon cracks form in association with the beginning of compressional yield. The cracks constitute water sills parallel to the thrust zone. Subsequent shear stress during weakening of the contact zone breaks bridges between cracks from different arrays, causing local displacement on a linked segment such as A–B–C–D. Subsidiary intracrystalline ductile deformation may occur in previously cemented veins.

Stage 3 represents the stage immediately following propagation of slip towards the foreland. Shear stress, τ_{yx}, is locally relieved on the slipped segment, so that σ_1 reverts to bedding-parallel (Fig. 18, Stage 3). As the contact zone is now completely decoupled, stress transfer from layer A to layer B and hence differential stress in layer B are at a maximum. Precipitation of calcite and slow ductile deformation then ensue, with the ultimate effect of restoring coherence and impermeability to the contact zone and reinstatement of Stage 0 conditions.

This, then, completes the basic cycle of fluid infiltration, shear failure and incremental slip. The processes described could cause repeated propagation of the décollement, as long as layer B does not fail internally and fluid input is maintained.

Stage 4. Stage 4 is a variant of stage 3 in which the increased stress in layer B approaches the compressive strength of the layer (upper part of mechanical region III in Fig. 17). Layer B then yields by developing inclined arrays of bedding-parallel extension cracks (Fig. 18). The stresses, which are sub-critical, might be maintained indefinitely, allowing solution-transfer activity to cement the fractures and produce en échelon veins. The stresses would then ultimately relax to Stage 0 as described for Stage 3.

Stage 5. If the strain associated with development of crack-arrays in Stage 4 continues before the cracks and the B/A contact zone are fully cemented, the rock may pass into mechanical region IV, leading to a through-going shear failure of one of the arrays. This initiates a thrust-ramp fault above the recently propagated part of the décollement. Shear stress on the ramp then drops to the residual strength for frictional resistance, and elastic strain released by the stress drop causes a small initial displacement on the ramp and further local slip on the décollement (Fig. 18, Stage 5). Meanwhile, fluid pressure would fall due to drainage of décollement fluid up the ramp (fault-valve behaviour of Sibson, 1990). This would tend to stabilze the ramp, unless fluid pressure built up again before cementation. Once cementation has taken place, stress in layer B would have to rise to Stage 0 level (by ductile flow) before renewed fracturing and displacement could occur. This also tends to stabilize the ramp,

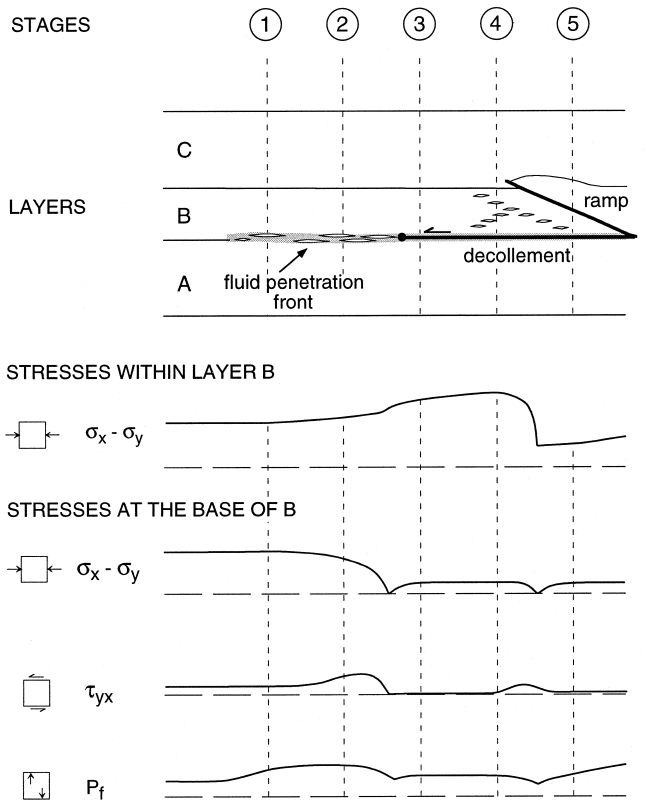

Fig. 21. Inferred lateral distribution of temporal stages described in Fig. 18, illustrating the mechanics of décollement propagation in a spatial frame.

because the next cycle begins with a lower stress in layer B than the previous cycle and is therefore more likely to end at Stage 3 (décollement propagation only). The ramps thus display self-regulatory behaviour, which limits their own development and promotes further propagation of the décollement.

It is emphasized that Stages 3–5 represent alternative end stages of a cycle. This implies that only propagation of the décollement (Stages 0–3) is an essential part of the model. In the model, movement on a hanging wall ramp is a possible but not essential consequence of this propagation, this being reflected in the fact that it is only one of the three possible end stages (Stage 5).

5.6. Spatial and temporal aspects of the model

The temporal sequence described above also has a spatial significance, as the different stages at a specific point may be equally considered as laterally adjacent states along the propagating décollement zone (Fig. 21). Stress cycling as envisaged in the model is compatible with seismic activity, with thrust movement by stick-slip increments. Horizontal cracks in compressional terrains usually precede seismic rupture (Sibson, 1989). In the Larra case cracks did not only evolve into high-angle reverse faults, but into a bedding décollement. Slip preceding Stages 3 and 5 was probably accompanied by seismic pulses, and separated by intervening periods of stress re-equilibration and distributed deformation. However, in active fault systems it has been observed that slip does not occur along the entire fault surface at the same time, but on discrete portions. This concept has been applied to thrust tectonics by De Bremaecker (1987) and Price (1988). The sequence of events proposed here may have been repeated as small increments at different times and in different places along the Larra thrust, eventually sweeping the entire surface. Local stress perturbations between slipped and non-slipped regions or elastic rebound may have been accommodated by high-angle extensional-veins which are present in the fault zone (i.e. B″, K, M, N and Q). Repetition of these processes is thought to have resulted in the complex superposition of structures observed in the Larra thrust zone.

6. Discussion and conclusions

The model proposed accounts for the development of décollement within a mechanically strong limestone unit, in preference to more easily flowing layers nearby. The Larra thrust was created by fluid channelling at a particular stratigraphical level, marked by a slight lithologic change within the limestone. Fluid channelling caused episodic brittle weakening and localized yield. Yield initially took the form of bedding-parallel extensional fractures, and the décollement was a channelway that largely controlled fluid flow through the sequence. The fault rock presently observable at the thrust zone consists of a dense stack of bedding- and thrust-parallel calcite veins, which show a variable degree of internal deformation (essentially by twinning) and recrystallization. Host-rock between veins shows moderate deformation, essentially by pressure-solution processes. Calcite textures indicate that each of the veins formed by a single process of dilatant opening followed by cementation. Thrust-parallel veins are so dense (sometimes constituting 100% of the rock) that they impart a strong foliation, which is subsidiarily marked by grain-size variations related to syntectonic recrystallization. Minor oblique veins also occur, and may be attributed either to shear between slipped and non-slipped portions of the thrust surface at a particular time increment, or to elastic rebound after slip.

The popular but perhaps over-used hydraulic fracture model is not applicable to the Larra thrust because of the relatively high stress to which the Cretaceous limestone was submitted, and because of the great number and proximity of the veins, which demands an extreme persistence of the process.

Individual veins were not formed by the repetition of small-aperture increments (crack–seal texture is lacking), but most appear created during a single event. A more effective mechanism for generating veins under these circumstances is suggested to be en échelon array geometry associated with shear failure in compression (the 'compressional fracture model'). That is to say, the development of extension-veins does not depend solely on high fluid pressure. Experimental work on the brittle–ductile transition in Solnhofen limestone under triaxial compression (Rutter, 1972) would appear to corroborate this view. At temperatures (200°C) not far from those of the study area, the transition occurs at high differential stress (~200 MPa at experimental strain rates) and between 0.90 and 1.00 fluid/confining pressure ratio (λ): i.e. under positive effective pressure.

Nevertheless we adapt part of Fyfe et al.'s (1978) and Cosgrove's (1993) models—namely the idea of 'fluid lenses' or 'water sills'—to explain subsequent behaviour of open fractures at the décollement horizon. Being constituted by interfaces between solid and fluid, these structures are surfaces of zero shear strength. Therefore the shear strength of the assembly is both much reduced and highly anisotropic as a result of their presence, particularly in the Larra case, where they must have been metric in length or greater. Thus, during subsequent décollement movement, displacement would be accommodated not by the arrays themselves, but by linkage of water sills and partially cemented veins from different arrays. This process could be effective in accommodating appreciable increments of slip during short time spans. Although there is no record of the magnitude of these increments, they would certainly be much greater than the 10–100 μm jumps typical of crack–seal shear veins (e.g. Labaume et al., 1991) and much faster than diffusion-accommodated sliding (Elliott, 1976), though the latter process may have been active at other times of the cycle.

The Larra thrust combines features of brittle (veining) and ductile (twinning, recrystallization and pressure-solution) deformation. In this respect is different from other carbonate fault rocks described in the literature that involve either extensive cataclasis (e.g. House and Gray, 1982; Ghisetti, 1987; Arboleya, 1989, etc.) or ductile shear of country rocks (e.g. Schmid, 1975; Heitzmann, 1987; Burkhard, 1990; Van der Pluijm, 1991, etc.). Alternation between brittle and ductile behaviour in thrust zones was also described by Wojtal and Mitra (1986), where ductile (diffusional) deformation was concentrated in the cataclastically refined matrix of the fault rock. In the Larra thrust, fine cataclasite is not observed. Intracrystalline deformation was concentrated in coarse-grained vein calcite, and in this respect it bears analogies to a thrust zone recently described by Kennedy and Logan (1997), a feature earlier reported in granitic rocks by Segall and Simpson (1986) who presented examples where ductile shearing was localized on mineralized dilatant fractures.

Mechanical models of thrust faulting account for shear failure on surfaces oblique to the main compressive stress, assisted by fluid reduction of the normal stresses. Reverse faulting is readily explained in this way. In the Larra thrust example, bedding-parallel veins are compatible with subhorizontal σ_1 in a thrust regime, but as major displacement was parallel to bedding (a décollement sensu stricto), the mechanics of its formation departed from simple models. In addition, as Segall and Simpson (1986) recognized, shearing parallel to preexisting extensional fractures requires some sort of stress reorientation to impart a shear stress on the fracture. If this may have happened through separate deformation events in the Segall and Simpson's examples, it must have occurred in a cyclic way in the Larra thrust. To account for this, the proposed model combines cyclic episodes of 1) bedding-parallel stress and cracking and 2) differential elastic contraction with forelandward decrease of horizontal compressive stress in the hanging wall and creation of subhorizontal shear stress at the contact, to maintain equilibrium of forces.

Even though twinning and recrystallization are conspicuous at the thin section scale, these were not key mechanisms in movement of the Larra thrust. Twinning by itself can account only for modest shear strains (less than $\gamma = 1$), and when combined with subsidiary dislocation creep leads to slightly greater values, but still moderate (e.g. Schmid et al., 1987). These are clearly insufficient to account for the kilometric displacement of the thrust with the present thickness of the shear zone. We conclude that displacement was mostly accommodated by slip on the water sills leaving little brittle signature, and that the fault can be classified as dominantly brittle, in spite of conspicuous ductile deformation at the grain scale.

It should be kept in mind that the Larra thrust did not form at the near-surface, but under several thousand meters of syntectonic sediments. Assuming a geothermal gradient of 30°C/km, the estimated burial suggests a temperature of deformation probably in excess of 200°. This order of temperature is lower than that experimentally calibrated for effective dislocation creep in calcite (Rutter, 1974; Schmid et al., 1987). However, the coexistence of fracturing and recrystallization during low-temperature deformation of carbonates is also described by Newman and Mitra (1994) and Kennedy and Logan (1997). At natural strain rates, recrystallization may occur at lower temperatures than those extrapolated from experiments, as other factors such as interstitial water have little influ-

ence on the intracrystalline deformation of coarse-grained calcite rocks (Rutter, 1974).

Observations of the Larra thrust indicate that sedimentary strata of the southern Pyrenees detached from the underlying basement despite the inconvenience posed by the absence of weak glide horizons at particular segments of the orogen. In the Pyrenees, basement ramps turn into bedding-décollements normally when they encounter Triassic evaporites. However, even where these soft rocks are absent, the Larra thrust demonstrates that basement ramps do not climb to the surface either, but still manage to flatten off at the base of the layered sequence. Décollement is then determined by the layered nature of the rocks themselves, which introduces vertical changes of viscosity which favour stress and fluid channelling that eventually result in décollement.

Acknowledgements

We thank T. Engelder for revision of the original manuscript. The comments by journal reviewers J. Casey Moore and S. Wojtal and by J. Cosgrove have also been most helpful. A. Teixell and M. L. Arboleya received financial support from DGICYT Project PB94-0685. D. W. Durney thanks the Generalitat de Catalunya, DGICYT, and Macquarie University for visits that facilitated fieldwork and collaboration.

References

Arboleya, M.L., 1989. Fault rocks of the Esla Thrust (Cantabrian Mountains, N Spain): an example of foliated cataclasites. Annales Tectonicae 3, 99–109.

Bolton, M., 1979. A guide to soil mechanics. Macmillan, London.

Brace, W.F., Paulding, B.W., Scholz, C., 1966. Dilatancy in the fracture of crystalline rocks. Journal of Geophysical Research 71, 3939–3953.

Burchfiel, B.C., Wernicke, B., Willemin, J.H., Axen, G.J., Cameron, C.S., 1982. A new type of décollement thrusting. Nature 300, 513–515.

Burkhard, M., 1990. Ductile deformation mechanisms in micritic limestones naturally deformed at low temperatures (150–350°C). In: Knipe, R.J., Rutter, E.H. (Eds.), Deformation Mechanisms, Rheology and Tectonics, Geological Society Special Publication 54, pp. 241–257.

Burkhard, M., 1993. Calcite twins, their geometry, appearance and significance as stress–strain markers and indicators of tectonic regime: a review. Journal of Structural Geology 15, 351–368.

Buxtorf, A., 1916. Prognosen und Befunde beim Hauensteinbasin— und Grenchenbergtunnel und die Bedeutung der letzeren für die Geologie des Juragebirges. Verhandl. Naturforsch. Gesellschaft Basel 27, 184–254.

Coleman Jr, J.L., Lopez, J.A., 1986. Dolomite décollements—Exception or rule? (abs.). American Association of Petroleum Geologists Bulletin 70, 576.

Cosgrove, J.W., 1993. The interplay between fluids, folds and thrusts during the deformation of a sedimentary succession. Journal of Structural Geology 15, 491–500.

Cox, S.F., 1987. Antitaxial crack-seal vein microstructures and their relationships to displacement paths. Journal of Structural Geology 9, 779–787.

Davis, D.M., Engelder, T., 1985. The role of salt in fold-and-thrust belts. Tectonophysics 119, 67–88.

De Bremaecker, J.Cl., 1987. Thrust sheet motion and earthquake mechanisms. Earth and Planetary Science Letters 83, 159–166.

De Roo, J.A., Weber, K., 1992. Laminated veins and hydrothermal breccia as markers of low-angle faulting, Rhenish Massif, Germany. Tectonophysics 208, 413–430.

Deere, D.U., 1968. In: Stagg, K.G., Zienkiewicz, O.C. (Eds.), Rock mechanics in engineering practice. Wiley, London, pp. 1–20.

Durney, D.W., 1972a. Deformation history of the Western Helvetic nappes. Ph.D. thesis, University of London.

Durney, D.W., 1972b. Solution-transfer, an important geological deformation mechanism. Nature 235, 315–317.

Durney, D.W., Kisch, H.J., 1994. A field classification and intensity scale for first-generation cleavages. AGSO Journal of Australian Geology & Geophysics 15, 257–295.

Elliott, D., 1976. The energy balance and deformation mechanisms of thrust sheets. Philosophical Transactions of the Royal Society of London A 283, 289–312.

Etheridge, M.A., 1983. Differential stress magnitudes during regional deformation and metamorphism: upper bonds imposed by tensile fracturing. Geology 11, 231–234.

Ferrill, D.A., Groshong, R.H., 1993. Kinematic model for the curvature of the northern Subalpine Chain, France. Journal of Structural Geology 15, 523–541.

Frederich, J.T., Evans, B., 1989. Micromechanics of the brittle to plastic transition in Carrara marble. Journal of Geophysical Research 94, 4129–4145.

Fyfe, W.S., Price, N.J., Thompson, A.B., 1978. Fluids in the earth's crust. Elsevier, Amsterdam.

Ghisetti, F., 1987. Mechanisms of thrust faulting in the Gran Sasso chain, Central Apennines, Italy. Journal of Structural Geology 9, 955–967.

Gramberg, J., 1965. Axial cleavage fracturing, a significant process in mining and geology. Engineering Geology 1, 31–72.

Hallbauer, D.K., Wagner, H., Cook, N.G.W., 1973. Some observations concerning the microscopic and mechanical behaviour of quartzite in stiff, triaxial compression tests. International Journal of Rock Mechanics, Mining Science and Geomechanics Abstracts 10, 713–726.

Heitzmann, P., 1987. Calcite mylonites in the Central Alpine ''root zone''. Tectonophysics 135, 207–215.

Henderson, J.R., Henderson, M.N., Wright, T.O., 1990. Water-sill hypothesis for the origin of certain veins in the Meguma Group, Nova Scotia, Canada. Geology 18, 654–657.

Hervouèt, Y., 1997. Déformations alpines, inversion tectonique négative et karstogenèse: exemple de la Pierre Saint-Martin (Pyrénées-Atlantiques, France). Bulletin de la Société géologique de France 168, 663–674.

House, W.H., Gray, D.R., 1982. Cataclasites along the Saltville thrust, U.S.A. and their implications for thrust sheet emplacement. Journal of Structural Geology 4, 257–269.

Hubbert, M.K., Rubey, W.W., 1959. Role of fluid pressure in the mechanics of overthrust faulting. Parts I and II. Geological Society of America Bulletin 70, 115–205.

Jaeger, J.C., Cook, N.G.W., 1969. Fundamentals of rock mechanics. Methuen, London.

Julivert, M., Arboleya, M.L., 1984. A geometrical and kinematical approach to the nappe structure in an arcuate fold belt: the Cantabrian nappes (Hercynian chain, NW Spain). Journal of Structural Geology 6, 499–519.

Kennedy, L.A., Logan, J.M., 1997. The role of veining and dissolution in the evolution of fine-grained mylonites: the McConnell thrust, Alberta. Journal of Structural Geology 19, 785–797.

Labaume, P., Séguret, M., Seyve, C., 1985. Evolution of a turbiditic foreland basin and analogy with an accretionary prism. Tectonics 4, 661–685.

Labaume, P., Berty, C., Laurent, P., 1991. Syn-diagenetic evolution of shear structures in superficial nappes: an example from the Northern Apennines (NW Italy). Journal of Structural Geology 13, 385–398.

Moore, J.C., 1989. Tectonics and hydrogeology of accretionary prisms: role of the décollement zone. Journal of Structural Geology 11, 95–106.

Mirouse, R., 1966. Recherches géologiques dans la partie occidentale de la zone primaire axiale des Pyrénées. Memoires Service de la Carte Géologique de France.

Newman, J., Mitra, G., 1994. Fluid-influenced deformation and recrystallization of dolomite at low temperatures along a natural fault zone, Mountain City window, Tennessee. Geological Society of America Bulletin 106, 1267–1280.

Olsson, W.A., Peng, S.S., 1976. Microcrack nucleation in marble. International Journal of Rock Mechanics, Mining Science and Geomechanics Abstracts 13, 53–59.

Paterson, M.S., 1978. Experimental rock deformation: the brittle field. Springer-Verlag, Berlin.

Pfiffner, O.A., 1993. The structure of the Helvetic nappes and its relation to the mechanical stratigraphy. Journal of Structural Geology 15, 511–521.

Phillips, W.J., 1972. Hydraulic fracturing and mineralisation. Journal of the Geological Society of London 128, 337–359.

Pierce, W.G., 1957. Heart Mountain and south Fork detachment thrusts of Wyoming. American Association of Petroleum Geologists Bulletin 41, 591–626.

Price, R.A., 1988. The mechanical paradox of large overthrusts. Geological Society of America Bulletin 100, 1898–1908.

Ramsay, J.G., 1967. Folding and fracturing of rocks. McGraw-Hill, New York.

Ramsay, J.G., 1981. Tectonics of the Helvetic nappes. In: McClay, K.R., Price, N.J. (Eds.), Thrust and nappe tectonics, Geological Society Special Publication 9, pp. 293–309.

Ramsay, J.G., Huber, M.I., 1987. The Techniques of Modern Structural Geology. Volume 2: Folds and Fractures. Academic Press, London.

Ribis, R., 1965. Contribution à l'étude géologique du Crétacé supérieur de la Haute-Chaîne dans la région de la Pierre-Saint-Martin (Basses-Pyrénées). Thèse 3ème Cycle, Université de Paris.

Rich, J.L., 1934. Mechanics of low-angle overthrust faulting as illustrated by Cumberland thrust block, Virginia, Kentucky and Tennessee. American Association of Petroleum Geologists Bulletin 18, 1584–1587.

Rodgers, J., 1949. Evolution of thought on structure of middle and southern Appalachians. American Association of Petroleum Geologists Bulletin 33, 1643–1654.

Rutter, E.H., 1972. The influence of interstitial water on the rheological behaviour of calcite rocks. Tectonophysics 14, 13–33.

Rutter, E.H., 1974. The influence of temperature, strain rate and interstitial water in the experimental deformation of calcite rocks. Tectonophysics 22, 311–334.

Schmid, S.M., 1975. The Glarus overthrust: field evidence and mechanical model. Eclogae Geologicae Helvetia 68, 247–280.

Schmid, S.M., Panozzo, R., Bauer, S., 1987. Special research paper: simple shear experiments on calcite rocks: rheology and microfabric. Journal of Structural Geology 9, 747–778.

Secor, D., 1965. Role of fluid pressure in jointing. American Journal of Science 263, 636–646.

Segall, P., Simpson, C., 1986. Nucleation of ductile shear zones in dilatant fractures. Geology 14, 56–59.

Séguret, M., 1972. Etude tectonique des nappes et séries décollées de la partie centrale du versant sud des Pyrénées. Caractère synsédimentaire, rôle de la compression et de la gravité. Thèse Doctorale, Université de Montpellier, Publ. USTELA. Série Géol. struct. 2.

Sibson, R.H., 1989. Earthquake faulting as a structural process. Journal of Structural Geology 11, 1–14.

Sibson, R.H., 1990. Conditions for fault-valve behaviour. In: Knipe, R.J., Rutter, E.H. (Eds.), Deformation Mechanisms, Rheology and Tectonics, Geological Society Special Publication 54, pp. 15–28.

Tapponnier, P., Brace, W.F., 1976. Development of stress-induced microcracks in granite. International Journal of Rock Mechanics, Mining Science and Geomechanics Abstracts 13, 103–112.

Teixell, A., 1990. Alpine thrusts at the western termination of the Pyrenean Axial zone. Bulletin de la Société géologique de France 8, 241–249.

Teixell, A., 1992. Estructura alpina en la transversal de la terminación occidental de la Zona Axial pirenaica. Tesis Doctoral, Universitat de Barcelona.

Teixell, A., 1996. The Ansó transect of the southern Pyrenees: basement and cover thrust geometries. Journal of the Geological Society, London 153, 301–310.

Thomas, A.L., Pollard, D.D., 1993. The geometry of en-échelon fractures in rock: implications from laboratory and numerical experiments. Journal of Structural Geology 15, 323–334.

Treagus, S.H., 1973. Buckling stability of a viscous single-layer system, oblique to the principal compression. Tectonophysics 19, 271–289.

Van der Pluijm, B.A., 1991. Marble mylonites in the Bancroft shear zone, Ontario, Canada: microstructures and deformation mechanisms. Journal of Structural Geology 13, 1125–1135.

Wawersik, W.R., Fairhurst, C., 1970. A study of brittle rock fracture in laboratory compression experiments. International Journal of Rock Mechanics, Mining Science and Geomechanics Abstracts 7, 561–575.

Wawersik, W.R., Brace, W.F., 1971. Post-failure behaviour of granite and diabase. Mechanics 3, 61–78.

Wibberley, C.A.J., 1997. Three-dimensional geometry, strain rates and basement deformation mechanisms of thrust-bend folding. Journal of Structural Geology 19, 535–550.

Wojtal, S., Mitra, G., 1986. Strain hardening and strain softening in fault zones from foreland thrusts. Geological Society of America Bulletin 97, 674–687.

Wong, T.-F., 1982. Micromechanics of faulting in Westerly granite. International Journal of Rock Mechanics, Mining Science and Geomechanics Abstracts 19, 49–64.

Woodward, N.B., Rutherford, E., 1989. Structural lithic units in external orogenic zones. Tectonophysics 158, 247–267.